HHS Public Access

Author manuscript

J Immunol. Author manuscript; available in PMC 2020 May 01.

Published in final edited form as:

J Immunol. 2019 May 01; 202(9): 2585–2608. doi:10.4049/jimmunol.1801350.

Effector and Activated T cells Induce Preterm Labor and Birth that is Prevented by Treatment with Progesterone[1]

Marcia Arenas-Hernandez[†,‡,§], **Roberto Romero**[†,¥,#,¶], **Yi Xu**[†,‡], **Bogdan Panaitescu**[‡], **Valeria Garcia-Flores**[†,‡], **Derek Miller**[†,‡], **Hyunyoung Ahn**[‡], **Bogdan Done**[†,‡], **Sonia S. Hassan**[†,‡,£], **Chaur-Dong Hsu**[‡], **Adi L. Tarca**[†,‡,Φ], **Carmen Sanchez-Torres**[§], and **Nardhy Gomez-Lopez**[†,‡,*,2]

[†]Perinatology Research Branch, NICHD/NIH/DHHS, Bethesda, MD, & Detroit, MI, USA

[‡]Department of Obstetrics & Gynecology, Wayne State University School of Medicine, Detroit, MI, USA

[§]Department of Molecular Biomedicine, CINVESTAV, Mexico City, MEX

[¥]Department of Obstetrics & Gynecology, University of Michigan, Ann Arbor, MI, USA

[#]Department of Epidemiology & Biostatistics, Michigan State University, East Lansing, MI, USA

[¶]Center for Molecular Obstetrics & Genetics, Wayne State University, Detroit, MI, USA

[£]Department of Physiology, Wayne State University School of Medicine, Detroit, Michigan, USA

[Φ]Department of Computer Science, Wayne State University College of Engineering, Detroit, Michigan, USA

[*]Department of Immunology & Microbiology, Wayne State University School of Medicine, Detroit, MI, USA

Abstract

Preterm labor commonly precedes preterm birth, the leading cause of perinatal morbidity and mortality worldwide. Most research has focused on establishing a causal link between innate immune activation and pathological inflammation leading to preterm labor and birth. However, the role of maternal effector/activated T cells in the pathogenesis of preterm labor/birth is poorly understood. Herein, we first demonstrated that effector memory and activated maternal T cells expressing granzyme B and perforin are enriched at the maternal-fetal interface (decidua) of women with spontaneous preterm labor. Next, using a murine model, we reported that prior to

[1]This research was supported, in part, by the Perinatology Research Branch (PRB), Division of Intramural Research, Eunice Kennedy Shriver National Institute of Child Health and Human Development, National Institutes of Health, U.S. Department of Health and Human Services (NICHD/NIH/DHHS), and, in part, with federal funds from the NICHD/NIH/DHHS under Contract No.HHSN275201300006C. This research was also supported by the Wayne State University Perinatal Initiative in Maternal, Perinatal and Child Health.

[2]**Address correspondence to:** Nardhy Gomez-Lopez, PhD; Department of Obstetrics and Gynecology, Wayne State University School of Medicine, Perinatology Research Branch, NICHD/NIH/DHHS, Detroit, Michigan 48201, USA, Tel (313) 577-8904, nardhy.gomez-lopez@wayne.edu; ngomezlo@med.wayne.edu.

[3]Non-standard abbreviations: CCL2, C-C motif chemokine ligand; CXCL, C-X-C motif chemokine ligand; G-CSF, colony stimulating factor 3; dpc, days post coitum; P4, progesterone; PTL, preterm labor; PTNL, preterm no labor; SO, sesame oil; TIL, term in labor; TNL, term no labor; αCD3, anti-CD3

inducing preterm birth, *in vivo* T-cell activation caused maternal hypothermia, bradycardia, systemic inflammation, cervical dilation, intra-amniotic inflammation, and fetal growth restriction, all of which are clinical signs associated with preterm labor. *In vivo* T-cell activation also induced B-cell cytokine responses, a pro-inflammatory macrophage polarization, and other inflammatory responses at the maternal-fetal interface and myometrium in the absence of an increased influx of neutrophils. Lastly, we showed that treatment with progesterone can serve as a strategy to prevent preterm labor/birth and adverse neonatal outcomes by attenuating the pro-inflammatory responses at the maternal-fetal interface and cervix induced by T-cell activation. Collectively, these findings provide mechanistic evidence showing that effector and activated T cells lead to pathological inflammation at the maternal-fetal interface, in the mother, and in the fetus prior to inducing preterm labor and birth and adverse neonatal outcomes. Such adverse effects can be prevented by treatment with progesterone, a clinically approved strategy.

INTRODUCTION

Preterm birth, delivery before 37 weeks of gestation, is the leading cause of perinatal morbidity and mortality worldwide (1, 2). Nearly two-thirds of all cases of preterm birth are preceded by spontaneous preterm labor (3–5), a syndrome of multiple pathological processes (6, 7). Of all the putative causes associated with spontaneous preterm labor, only pathological inflammation has been causally linked to preterm birth (8–12).

Pathological inflammation can be triggered by pathogen-associated molecular patterns (PAMPs) or damage-associated molecular patterns (DAMPs) (i.e. alarmins) (13–16). PAMPs and DAMPs are sensed by pattern recognition receptors (PRRs), which are mainly present in innate immune cells (17). Therefore, most of the perinatal immunology research has focused on the role of innate immunity in the mechanisms that lead to preterm labor (18–31). Indeed, the stimulation of neutrophils/macrophages by administration of an endotoxin (32, 33) or activation of invariant natural killer T cells via alpha-galactosylceramide (34, 35) induces preterm labor and birth. However, pathological inflammation can also be mediated by T cells, the cellular component of the adaptive immune system (36). T cells have been implicated in implantation (37–40) and pregnancy maintenance through the mediation of maternal-fetal tolerance (41–56), and their infiltration at the maternal-fetal interface (i.e. decidua) has been associated with the physiological process of labor at term (57–61) and the syndrome of preterm labor and birth (62–64). However, a mechanistic link between maternal T cells and the pathophysiology of preterm labor and birth is lacking.

Herein, we hypothesized that effector/activated T cells can trigger the mechanisms leading to preterm labor and birth. This proposal is based on the clinical observation that chronic chorioamnionitis, a placental lesion in which maternal T cells infiltrate the fetal tissues (e.g. chorioamniotic membranes) through the decidua (64), is strongly associated with preterm labor and birth (62), and women with this condition display a systemic T-cell mediated cytotoxicity (65). In line with this hypothesis, it was also shown that transcriptional silencing limits the infiltration of T cells and other immune cells into the maternal-fetal interface (66–68), suggesting that an uncontrolled invasion of effector T cells may lead to pregnancy complications. More recently, we provided further evidence supporting a link between

maternal T cells and preterm labor/birth by injecting an αCD3ε antibody, which is capable of inducing T-cell activation (69–71) and preterm labor/birth (72). However, the mechanisms whereby maternal T-cell activation induces preterm birth, and whether such an effect can be prevented, are unknown.

Herein, we aimed to determine whether effector T cells at the maternal-fetal interface are associated with spontaneous preterm labor (humans) and to investigate the mechanisms (murine animal models) whereby the activation of such immune cells induce pathological inflammation leading to preterm birth and adverse neonatal outcomes. Furthermore, we proposed the use of an approved therapeutic approach, progesterone, to prevent T-cell activation-induced preterm labor/birth and its adverse neonatal outcomes.

MATERIALS AND METHODS

Human subjects, clinical specimens, and definitions

Human placental basal plate (decidua basalis) and chorioamniotic membrane (decidua parietalis) samples were obtained at the Perinatology Research Branch, an intramural program of the *Eunice Kennedy Shriver* National Institute of Child Health and Human Development (NICHD), National Institutes of Health, U. S. Department of Health and Human Services, Wayne State University (Detroit, MI, USA), and the Detroit Medical Center (Detroit, MI, USA). The collection and utilization of human materials for research purposes were approved by the Institutional Review Boards of the NICHD and Wayne State University. All participating women provided written informed consent. The study groups included women who delivered at term with (TIL) or without (TNL) spontaneous labor or preterm with (PTL) or without (PTNL) spontaneous labor. Two separate cohorts of women were used in this study: one for the immunophenotyping of effector T cells and one for the immunophenotyping of activated T cells. The demographic and clinical characteristics of the study groups are shown in Tables I and II. Labor was defined by the presence of regular uterine contractions at a frequency of at least two contractions every 10 min with cervical changes resulting in delivery. Preterm delivery was defined as delivery <37 weeks of gestation. Patients with multiple births or neonates that had congenital or chromosomal abnormalities were excluded.

Decidual leukocyte isolation from human samples

Decidual leukocytes from human decidual tissue were isolated as previously described (73). Briefly, the decidua basalis was collected from the basal plate of the placenta, and the decidua parietalis was separated from the chorioamniotic membranes. Decidual tissue was homogenized using a gentleMACS Dissociator (Miltenyi Biotec, San Diego, CA, USA) in StemPro Cell Dissociation Reagent (Life Technologies, Grand Island, NY, USA). Homogenized tissues were incubated for 45 min at 37°C with gentle agitation. After incubation, tissues were washed with ice-cold 1X PBS and filtered through a 100 μm cell strainer. Cell suspensions were collected and centrifuged at 300 x g for 10 min at 4ºC, and the cell pellet was suspended in stain buffer (Cat#554656; BD Biosciences, San Jose, CA, USA). Mononuclear cells were purified using a density gradient (Ficoll-Paque Plus; GE Healthcare Bio-Sciences, Uppsala, Sweden), following the manufacturer's instructions.

Lastly, mononuclear cell suspensions were washed using stain buffer before immunophenotyping.

Immunophenotyping of human decidual leukocytes

Mononuclear cell suspensions from decidual tissues were stained with BD Horizon Fixable Viability Stain 510 dye (BD Biosciences) prior to incubation with extracellular and intracellular mAbs. Mononuclear cell suspensions were washed with stain buffer and centrifuged. Cell pellets were incubated for 10 min with 20 μl of human FcR Blocking Reagent (Miltenyi Biotec) in 80 μl of stain buffer. Next, mononuclear cell suspensions were incubated with extracellular fluorochrome-conjugated anti-human mAbs (Supplementary Table I) for 30 min at 4ºC in the dark. After extracellular staining, the cells were fixed. For intracellular staining, the cells were fixed and permeabilized using the BD Cytofix/Cytoperm Fixation/Permeabilization kit (BD Biosciences) prior to incubation with intracellular antibodies (Supplementary Table I). Finally, mononuclear cell suspensions were washed and resuspended in 0.5 mL stain buffer and acquired using the BD LSRFortessa flow cytometer and FACSDiva 6.0 software. Leukocyte subsets were gated within the viability gate. Immunophenotyping included the identification of: effector memory T cells (T_{EM}; CD3+CD4+ or CD3+CD4− CD45RA−CCR7−), naïve T cells (T_N; CD3+CD4+ or CD3+CD4− CD45RA+CCR7+), central memory T cells (T_{CM}; CD3+CD4+ or CD3+CD4− CD45RA−CCR7+), and effector memory RA T cells (T_{EMRA}; CD3+CD4+ or C3+CD4− CD45RA+CCR7−). Activated CD4+ and CD8+ T cells were evaluated by the expression of granzyme B and/or perforin. The data analysis was performed using FlowJo software v10 (TreeStar, Ashland, OR, USA).

Determination of decidual T-cell origin

Human placental basal plate (decidua basalis) and chorioamniotic membranes (decidua parietalis) were obtained from women who delivered a male neonate and decidual leukocytes were isolated as described above. Case-matched umbilical cord blood and maternal peripheral blood samples were also obtained and mononuclear cells were purified using a density gradient (Ficoll-Paque Plus), following the manufacturer's instructions. Next, T cells were isolated from decidual, cord blood, and maternal mononuclear cells by magnetic separation using the human REAlease CD3 MicroBead kit (Miltenyi Biotec) and MS magnetic columns (Miltenyi Biotec), following the manufacturer's instructions. After separation, isolated T cells were counted using an automatic cell counter (Cellometer Auto 2000; Nexcelom Bioscience, Lawrence, MA, USA), and the purity (>95%) of the isolated T cells was assessed by flow cytometry using a fluorochrome-conjugated anti-human monoclonal anti-CD3 antibody (Cat#564307; BD Biosciences). Purified T cells were then centrifuged at 500 x g for 5 min and the cell pellet was stored at −80°C until use.

Genomic DNA was extracted from isolated decidual, cord blood, and maternal CD3+ T cells using the QIAamp UCP DNA Micro kit (Qiagen, Hilden, Germany), following the manufacturer's instructions. DNA concentrations and purity were assessed with the NanoDrop 1000 spectrophotometer (Thermo Fisher Scientific, Wilmington, DE, USA). Quantitative PCR (qPCR) was performed using the ABI 7500 FAST Real-Time PCR System (Applied Biosystems, Life Technologies Corporation, Foster City, CA, USA). The TaqMan

assays used to detect a gene region on the Y chromosome or X chromosome were *SRY* (Y-chromosome) (Cat#Hs00976796_s1) and *AR* (X-chromosome) (Cat#Hs05033429_s1). As an internal control, the *18S* housekeeping gene was also detected (Cat#Hs9999901_s1). Each qPCR reaction contained 10 μL of 2X TaqMan Fast Advanced master mix (Cat#444553, Thermo Fisher Scientific), 1 μL of the TaqMan assay, and 9 μL of genomic DNA (2 ng total) to yield a 20 μL reaction, and each sample was run in duplicate. The thermal cycling profile began with 95ºC for 10 minutes, followed by 40 cycles of 95ºC for 15 seconds and 60ºC for 1 minute. Ct values for the *SYR*, *AR*, and *18S* qPCRs were generated using the ABI 7500 Fast System SDS software version 1.3 (Applied Biosystems). The formula used to calculate the *SYR*/*AR* qPCR signal ratio for each sample was: $2^{-(\Delta Ct(SRY-18S)-\Delta Ct(AR-18S))} = 2^{-\Delta\Delta Ct}$.

PCR amplification of the *SRY* gene was also performed using the traditional PCR technique. The primers used to amplify the *SRY* region were *SRY*-forward (5'-GGTGTTGAGGGCGGAGAAATGC-3') (100 nM) and *SRY*-reverse (5'-GTAGCCATTGTTACCCGATTGTC-3' (100 nM). The internal control β-Globin (*HBB*), was amplified using β-globin forward (5'-GCTTCTGACACAACTGTGTTCACTAGC-3') (200 nM) and β-globin reverse (5'-CACCAACTTCATCCACGTTCACC-3') (200 nM) primers. The PCR reaction included 25 μL of 2X PCR master mix (Cat#K0171, Thermo Fisher Scientific), 1 μL each of the forward and reverse primers (at concentrations indicated above), and 21 μL of genomic DNA (50 ng total) to yield a 50 μL reaction. The thermal cycling profile for the PCR began with 94ºC for 5 minutes, followed by 30 cycles of 94ºC for 1 minute, 60ºC for 1 minute, and 72ºC for 1 minute. The results of the PCR reaction were visualized using gel electrophoresis with E-Gel General Purpose 2% Agarose (Cat#G501802, Thermo Fisher Scientific). The gel image was acquired using the ChemiDoc MP Imaging System (Bio-Rad, Hercules, CA, USA).

Mice

C57BL/6J mice were purchased The Jackson Laboratory (Bar Harbor, ME, USA) and bred in the animal care facility at the C.S. Mott Center for Human Growth and Development, Wayne State University, Detroit, MI, USA and housed under a circadian cycle (light:dark = 12:12 h). Eight- to twelve-week-old females were mated with males of proven fertility. Female mice were examined daily between 8:00 and 9:00 AM for the presence of a vaginal plug, which indicated 0.5 days *post coitum* (dpc). Upon observation of vaginal plugs, female mice were removed from the mating cages and housed separately. A weight gain ≥2g confirmed pregnancy at 12.5 dpc. All animal experiments were approved by the Institutional Animal Care and Use Committee at Wayne State University (Protocol No. A-09–08-12, A-07–03-15, and 18–03-0584). The authors adhered to the NIH Guide for the Care and Use of Laboratory Animals.

Animal models of preterm labor and birth

Anti-CD3ε-induced preterm labor/birth (72). Dams were injected intraperitoneally (i.p.) with 10μg/200μL of a monoclonal anti-CD3ε antibody (αCD3ε) (Clone 145–2C11; BD Biosciences) dissolved in sterile 1X phosphate-buffered saline (PBS) (Fisher Scientific Chemicals, Fair Lawn, NJ, USA) using a 26-gauge needle on 16.5 dpc. Controls were i.p.

injected with 10μg/200μL of IgG1 κ isotype control (Clone A19–3; BD Biosciences) dissolved in sterile 1X PBS. N = 4 – 7 each.

LPS-induced preterm labor/birth (32, 74). Dams were injected i.p. with 15μg/150μL of LPS (*Escherichia coli* 055:B5; Sigma-Aldrich, St Louis, MO, USA) dissolved in sterile 1X PBS using a 26-gauge needle on 16.5 dpc. Controls were injected with 150μL of sterile 1X PBS alone. N = 7 – 8 each.

RU486-induced preterm labor/birth (75). Dams were injected subcutaneously (s.q.) with 150μg/100μL of RU486 (Mifepristone) (Sigma Aldrich) dissolved in dimethyl sulfoxide (DMSO) (Sigma-Aldrich) and diluted 1:13 in sterile 1X PBS or 100μL of DMSO diluted 1:13 in sterile 1X PBS as a control on 15.5 dpc. N = 3 – 8 each.

Following injection, pregnant mice were monitored using a video camera with infrared light (Sony, Tokyo, Japan) until delivery. Gestational length was calculated from the presence of the vaginal plug (0.5 dpc) until the observation of the first pup in the cage bedding. Preterm birth was defined as delivery <18.0 dpc.

Determination of body temperature

To determine body temperature, dams were injected with either αCD3ε, LPS, or RU486 (or their respective controls) (n = 5 each). Prior to injection the basal body temperature was taken using a rectal probe (TMH-150; VisualSonics Inc., Toronto, ON, Canada) and represented time zero. Following injection, the body temperature was recorded every 2 h until 12 h post-injection.

Determination of maternal heart rate using high-frequency ultrasound

Dams were injected with αCD3ε, LPS, or RU486 (or their respective controls) (n = 13 – 17 each for αCD3ε, 8 – 11 each for LPS, and 6 – 7 each for RU486). Twelve hours post-injection, each pregnant mouse underwent ultrasound assessment as previously described (34, 72, 74, 76–78). Briefly, mice were anesthetized by inhalation of 2–3% isoflurane (Aerrane; Baxter Healthcare Corporation, Deerfield, IL, USA) and 1–2 L/min oxygen in an induction chamber. Mice were then positioned on a heated platform and stabilized using adhesive tape and fur was removed from the abdomen and thorax. Body temperature was maintained at 37±1°C and monitored using a rectal probe. A 55 MHz linear ultrasound probe (VisualSonics Inc., Toronto, ON, Canada) was fixed and mobilized with a mechanical holder, and the transducer was slowly moved toward the abdomen. The maternal heart rate was calculated using three similar consecutive waveforms from the uterine artery. Ultrasound signals were processed, displayed, and stored using the Vevo Imaging Station (VisualSonics Inc).

Determination of cervical dilation

Dams were injected with αCD3ε, LPS, or RU486 (or their respective controls) (n = 8 each). Mice were euthanized 12–16 h post-injection and cervical tissues were collected, photographed, and blindly measured to determine cervical width as a surrogate of cervical dilation.

Leukocyte isolation from murine decidual, myometrial, and lymphatic tissues

Dams were injected with αCD3ε, LPS, or RU486 (or their respective controls) (n = 10 – 13 each for αCD3ε, 8 – 10 each for LPS, and 9 – 10 each for RU486). Mice were euthanized 12–16 h post-injection and decidual and myometrial tissues from the implantation sites were collected. Isolation of leukocytes from decidual and myometrial tissues was performed, as previously described (79). Briefly, tissues were cut into small pieces using fine scissors and enzymatically digested with StemPro Cell Dissociation Reagent for 35 minutes at 37°C. The spleen and uterine lymph nodes (ULN) were also collected and leukocyte suspensions were prepared, as previously reported (32). Leukocyte suspensions were filtered using a 100 μm cell strainer and washed with FACS buffer [0.1% BSA (Sigma-Aldrich) and 0.05% sodium azide (Fisher Scientific Chemicals) in 1X PBS] before immunophenotyping.

Immunophenotyping of decidual, myometrial, and lymphatic leukocytes

Leukocyte suspensions from decidual, myometrial, and lymphatic tissues were centrifuged at 1250 x g for 10 min at 4ºC. Cell pellets were then incubated with the CD16/CD32 monoclonal antibody (mAb) (FcγIII/II Receptor; BD Biosciences) for 10 minutes and subsequently incubated with specific fluorochrome-conjugated anti-mouse mAbs (Supplementary Table I) for 30 min at 4°C in the dark. Leukocyte suspensions were fixed/permeabilized with the BD Cytofix/Cytoperm Fixation/Permeabilization kit prior to staining with intracellular antibodies. Cells were acquired using the BD LSRFortessa flow cytometer and FACSDiva 8.0 software. Immunophenotyping included the identification of T cells (CD3+CD4+ and CD3+CD8+ cells) and their activation status by the expression of CD25, CD69, CD44, CD62L, CTLA-4 (CD152), PD-1 (CD279), IL2, and IFNγ in the decidual, myometrial, and lymphatic tissues. B cells (CD45+CD19+) and their activation by the expression of IFNγ; M1- and M2-like macrophage phenotypes (CD11b+F4/80+iNOS+ or Arg1+IL10+); and neutrophils (CD45+F4/80-Ly6G+) were also determined in the decidual and myometrial tissues. Data were analyzed using FlowJo software v10.

Gene expression of M1 and M2 markers in decidual and myometrial macrophages

Dams were injected with αCD3ε, LPS, or RU486 (or their respective controls) (n = 6–8 per group). Mice were euthanized 12–16 h post-injection and decidual and myometrial tissues from the implantation sites were collected. Leukocytes were isolated from the decidual and myometrial tissues as described above. Leukocyte suspensions were sequentially filtered using a 100 μm cell strainer followed by a 30 μm cell strainer, and then washed with 1X PBS. After centrifugation at 300 x g for 10 min at 4 ºC, the leukocytes were resuspended in 1 mL of 1X PBS and counted using an automatic cell counter (Cellometer Auto 2000; Nexcelom Bioscience). Macrophages were then isolated from decidual and myometrial cells by magnetic separation using mouse Anti-F4/80 UltraPure MicroBeads (Miltenyi Biotec) and MS magnetic columns (Miltenyi Biotec), following the manufacturer's instructions. After elution from the column, a small aliquot of the isolated F4/80+ cells was taken to assess the purity by flow cytometry using the fluorochrome-conjugated anti-mouse monoclonal antibodies CD45, CD11b, and F4/80 (Supplementary Table I). Isolated F4/80+ cells were then centrifuged and the cell pellet was resuspended in 350 μL RLT Lysis Buffer (Qiagen). Total RNA was isolated from F4/80+ cells using the RNeasy micro kit (Qiagen),

following the manufacturer's instructions. RNA integrity was evaluated with the 2100 Bioanalyzer system (Agilent Technologies, Wilmington, DE, USA) using the Agilent RNA 6000 Pico Kit (Agilent Technologies). Complementary (c)DNA was synthesized by using the SuperScript® III First-Strand Synthesis System for RT-PCR (Invitrogen, Life Technologies, Carlsbad, CA, USA) on the Applied Biosystems GeneAmp PCR System 9700 (Applied Biosystems, Life Technologies, Foster City, CA, USA), following the manufacturer's instructions. Complementary DNA was amplified using the TaqMan® PreAmp Master Mix (2X) (Applied Biosystems) on the Applied Biosystems 7500 Fast Real-time PCR System. Messenger RNA expression was determined by quantitative real-time PCR (qRT-PCR) using a BioMark high-throughput qRT-PCR System (Fluidigm, San Francisco, CA, USA) and TaqMan® gene expression assays (Thermo Fisher) (Supplementary Table I).

Determination of pro-inflammatory and contractility-related genes in decidual and myometrial tissues

Dams were injected with αCD3ε, LPS, or RU486 (or their respective controls) (n = 7 – 9 each for αCD3ε, 9 – 13 each for LPS, and 11 – 16 each for RU486). Mice were euthanized 12–16 h post-injection and decidual and myometrial tissues from the implantation sites were collected and placed in RNA*later* Stabilization Solution (Life Technologies). Total RNA was isolated from decidual and myometrial tissues using the RNeasy mini kit (Qiagen), following the manufacturer's instructions. RNA concentrations and purity were assessed with the NanoDrop 1000 spectrophotometer (Thermo Scientific, Wilmington, DE, USA), and RNA integrity was evaluated with the 2100 Bioanalyzer system (Agilent Technologies) using the Agilent RNA 6000 Nano Kit (Agilent Technologies). Complementary (c)DNA was synthesized by using the SuperScript® III First-Strand Synthesis System for RT-PCR (Invitrogen, Life Technologies) on the Applied Biosystems GeneAmp PCR System 9700 (Applied Biosystems, Life Technologies), following the manufacturer's instructions. Complementary DNA was amplified using the TaqMan® PreAmp Master Mix (2X) (Applied Biosystems) on the Applied Biosystems 7500 Fast Real-time PCR System. Messenger RNA expression was determined by quantitative real-time PCR (qRT-PCR) using a BioMark high-throughput qRT-PCR System (Fluidigm) and TaqMan® gene expression assays (Thermo Fisher) (Supplementary Table I).

Determination of cytokine concentrations in amniotic fluid and the maternal circulation

Dams were injected with αCD3ε, LPS, or RU486 (or their respective controls). Mice were euthanized 12–16 h post-injection and peripheral blood was collected by cardiac puncture for serum separation (n = 11 – 12 each for αCD3ε, 10 each for LPS, and 10 each for RU486). Amniotic fluid was also obtained from each amniotic sac with a 26-gauge needle (n = 5 each for αCD3ε, 5 each for LPS, and 5 each for RU486). Maternal serum and amniotic fluid samples were centrifuged at 1300 x g for 10 min at 4°C and the supernatants were separated and stored at −20°C until analysis. The ProcartaPlex Mouse Cytokine & Chemokine Panel 1A 36-plex (Invitrogen by Thermo Fisher Scientific, Vienna, Austria) was used to measure the concentrations of IFNγ, IFNα, IL-12p70, IL1β, TNFα, GM-CSF, IL18, IL17A, IL22, IL23, IL27, IL9, IL15/IL15R, IL13, IL2, IL4, IL5, IL6, IL10, CCL11, IL28, IL3, LIF, IL1α, IL31, CXCL1, CCL3, CXCL10, CCL2, CCL7, CCL4, CXCL2, CCL5, G-

CSF, M-CSF, and CXCL5 in serum and amniotic fluid samples, according to the manufacturer's instructions. Plates were read using the Luminex 100 SystemFill (Luminex, Austin, TX, USA), and analyte concentrations were calculated with ProcartaPlex Analyst 1.0 Software from Affymetrix, San Diego, CA, USA. The sensitivities of the assays were: 0.09 pg/mL (IFNγ), 3.03pg/mL (IFNα), 0.21 pg/mL (IL12p70), 0.14 pg/mL (IL1β), 0.39 pg/mL (TNFα), 0.19 pg/mL (GM-CSF), 9.95 pg/mL (IL18), 0.08 pg/mL (IL17A), 0.24 pg/mL (IL22), 2.21 pg/mL (IL23), 0.34 pg/mL (IL27), 0.28 pg/mL (IL9), 0.42 pg/mL (IL15/IL15R), 0.16 pg/mL (IL13), 0.10pg/mL (IL2), 0.03 pg/mL (IL4), 0.32 pg/mL (IL5), 0.21 pg/mL (IL6), 0.69 pg/mL (IL10), 0.01 pg/mL (CCL11), 20.31 pg/mL (IL28), 0.11 pg/mL (IL3), 0.28 pg/mL (LIF), 0.32 pg/mL (IL1α), 0.45 pg/mL (IL31), 0.05 pg/mL (CXCL1), 0.13 pg/mL (CCL3), 0.26 pg/mL (CXCL10), 3.43 pg/mL (CCL2), 0.15 pg/mL (CCL7), 1.16 pg/mL (CCL4), 0.37 pg/mL (CXCL2), 0.35 pg/mL (CCL5), 0.19 pg/mL (G-CSF), 0.02 pg/mL (M-CSF), and 5.67 pg/mL (CXCL5). Inter-assay and intra-assay coefficients of variation were less than 10%.

Cytokine concentrations in amniotic fluid were adjusted by protein concentration, which were determined using the Pierce™ BCA Protein Assay Kit (Pierce Biotechnology, Rockford, IL, USA), following the manufacturer's instructions.

Fetal growth parameters

Dams were injected with αCD3ε, LPS, or RU486 (or their respective controls) (n = 7 each for αCD3ε, 10 each for LPS, and 10 each for RU486). Mice were euthanized 12–16 h post-injection and representative images of the fetuses and placentas were obtained. Fetuses were also weighed followed by dissection to obtain representative images of their lungs.

Hematoxylin and Eosin (H&E) and Masson's trichrome staining

The lungs of preterm and term neonates (n=3 each) were fixed in 4% paraformaldehyde for 24 h and stored at 4°C in ethanol prior to embedding in paraffin blocks. The embedded tissues were then cut into 5-μm-thick sections, placed onto salinized slides, deparaffinized with xylene, and hydrated with ethanol. Slides were stained with hematoxylin (Cat#88018, Thermo Scientific) for 10 s, washed with distilled water, and immersed in 80% ethanol followed by staining with eosin (Cat#71211, Thermo Scientific) for 10 s. The sections were then dehydrated in a series of alcohol baths and xylene, and a coverslip was applied. The Masson's trichrome staining was performed using the Masson's trichrome stain kit (American MasterTech, Lodi, CA, USA), according to the manufacturer's protocol. The sections were then dehydrated in a series of alcohol baths and xylene, and a coverslip was applied. All images were taken using the Vectra Polaris Quantitative Slide Scanner (Perkin Elmer, Waltham, MA, USA).

Determination of progesterone concentration in the maternal circulation

Dams were injected with αCD3ε or isotype control (n = 10 – 11 each). Mice were euthanized 16 h post-injection and peripheral blood was collected by cardiac puncture for serum separation. Maternal serum was centrifuged at 1300 x g for 10 min at 4°C and the supernatants were separated and stored at −20°C until analysis. Serum progesterone was measured using the PROG-EASIA ELISA kit (GenWay Biotech, Inc., San Diego, CA,

USA), according to the manufacturer's instructions. The sensitivity of the assay was 0.08 ± 0.03 ng/mL. The intra-assay coefficient of variation was 10.5%.

Preterm birth rescue by treatment with progesterone

Dams were injected s.q. with either 1 mg/200μL of progesterone (P4, Sigma-Aldrich) diluted in sesame oil (SO, Sigma-Aldrich) or 200 μL of sesame oil (control groups) on 15.5 dpc, 16.5 dpc, and 17.5 dpc. On 16.5 dpc, dams were also injected with either 10 μg/200 μL of αCD3ε or isotype control (n= 5 – 10 each). Following the last injection, dams were monitored via video camera with infrared light until delivery. The rate of preterm birth and gestational length was recorded as previously described. The rate of neonatal mortality was calculated as the number of pups found dead among the total litter size. Representative images of pups and their lungs just after birth and at 1 day old were also obtained.

Determination of pro-inflammatory genes in decidual, myometrial and cervical tissues after treatment with progesterone

Dams were injected s.q. with either 1 mg/200μL of progesterone (P4, Sigma-Aldrich) diluted in sesame oil (SO, Sigma-Aldrich) or 200 μL of sesame oil (control groups) on 15.5 dpc and 16.5 dpc. On 16.5 dpc, dams were also injected with either 10 μg/200 μL of αCD3ε or isotype control (n= 5 each). Approximately 16 h after αCD3ε or isotype injection, mice were euthanized and decidual and myometrial tissues from the implantation sites as well as cervical tissues were collected and placed in RNA*later* Stabilization Solution (Life Technologies). Total RNA was isolated from tissues using the RNeasy mini kit (Qiagen), following the manufacturer's instructions. RNA concentrations and purity were assessed with the NanoDrop 1000 spectrophotometer (Thermo Scientific), and RNA integrity was evaluated with the 2100 Bioanalyzer system (Agilent Technologies) using the Agilent RNA 6000 Nano Kit (Agilent Technologies). Complementary (c)DNA was synthesized by using the SuperScript® III First-Strand Synthesis System for RT-PCR (Invitrogen, Life Technologies) on the Eppendorf AG (Eppendorf, Hamburg, Germany), following the manufacturer's instructions. Complementary DNA was amplified using the TaqMan® PreAmp Master Mix (2X) (Applied Biosystems) on the Applied Biosystems 7500 Fast Real-time PCR System. Messenger RNA expression was determined by quantitative real-time PCR (qRT-PCR) using a BioMark high-throughput qRT-PCR System (Fluidigm) and TaqMan® gene expression assays (Thermo Fisher) (Supplementary Table I).

Statistics

Statistical analyses were performed using SPSS v19.0 (IBM Corporation, Armonk, NY, USA) or the R package (https://www.r-project.org/). For human demographic data, the group comparisons were performed using the Fisher's exact test for proportions and Kruskal–Wallis tests for non-normally distributed continuous variables. When proportions are displayed, percentages and 95% confidence intervals (CI) are shown. Medians are shown with the interquartile range (IQR). Kaplan-Meier survival curves were used to plot and compare the gestational length data (Mantel–Cox test). For maternal heart rates and fetal weights, the statistical significance of group comparisons was assessed using the *t* test and the means are shown with the standard error of the mean (SEM). For the rates of preterm birth and neonatal mortality, the Fisher's exact test was utilized. For body temperature,

cervical widths, multiplex, and ELISA and flow cytometry murine data, the statistical significance between groups was determined using a Mann–Whitney *U* test. For qRT-PCR arrays, negative ΔCt values were determined using multiple reference genes (*Gusb, Hsp90ab1, Gapdh, and Actb*) averaged within each sample to determine gene expression levels. Heat maps were created for the group mean expression matrix (gene x group mean), with each gene expression level being standardized first. The heat maps shown in Figures 5 & 6 represent the Z-scores of the mean (−ΔCt). The heat maps found in Figure 10 display the –ΔCt values of each group, centered on the –ΔCt value of the control group treated with sesame oil (SO) + Isotype. All heat maps show hierarchical clustering using correlation distance. The p-values were determined by unpaired *t*-test or Mann–Whitney *U* test. A p value of ≤ 0.05 was considered statistically significant.

RESULTS

Effector and activated maternal T cells are enriched at the human maternal-fetal interface during spontaneous preterm labor

Naïve T cells (T_N) travel throughout the circulation in search of antigens presented by dendritic cells (80). Upon antigen presentation, T cells proliferate and differentiate into effector cells that can migrate to B-cell areas or inflamed tissues (81). A proportion of these cells persist as circulating memory T cells conferring protection against the known antigen (82). Memory T cells can be subdivided based on their phenotype and function into central memory T cells (T_{CM}), which display high proliferative potential but lack an immediate effector function, and effector memory (T_{EM}) and terminally differentiated effector memory (T_{EMRA}) T cells that have low proliferative capacity but display rapid effector function (83, 84). Such cells can be distinguished by the expression of CD45RA, which is expressed by naïve or terminally differentiated T cells, and CCR7, a lymph node homing receptor (83, 84). We have previously shown that memory-like T cells with effector functions are present at the human maternal-fetal interface during the physiological process of term labor (58, 59). Therefore, using immunophenotyping, we first investigated whether the different effector T-cell subsets were differentially distributed in the decidual tissues of women with spontaneous preterm labor (Fig. 1A). Strikingly, both CD4+ and CD8+ T_{EM} were the most abundant T-cell subsets at the human maternal-fetal interface (i.e. decidua basalis and decidua parietalis) (Fig. 1B and Fig. S1A). Indeed, CD4+ and CD8+ T_{EM} were enriched at the maternal-fetal interface of women who underwent spontaneous preterm labor compared to those who delivered at term (Fig. 1B and Fig. S1A). The increase in T_{EM} was accompanied by a reduction in both CD4+ and CD8+ T_N (Fig. 1C) and T_{CM} (Fig. 1D) at the maternal-fetal interface of women with spontaneous preterm labor (Fig. 1C&D and Fig. S1B&C). CD8+ T_{EMRA} were also greater at the maternal-fetal interface of women who underwent spontaneous preterm labor compared to those who delivered preterm without labor (Fig. 1E and Fig. S1D).

After encountering their antigen, T_{EM} become activated and perform their effector functions through the release of inflammatory mediators such as granzyme B and perforin (85–89). Therefore, we next investigated whether effector T cells expressed granzyme B and perforin at the human maternal-fetal interface (Fig. 2A). Consistent with our previous findings, CD4+

and CD8+ T cells expressing granzyme B and perforin were enriched at the maternal-fetal interface of women with spontaneous preterm labor (Fig. 2B&C and Fig. S1E&F).

In order to confirm the maternal origin of T cells at the maternal-fetal interface, we measured the ratio of *SRY* (Y-chromosome) to *AR* (X-chromosome) expression in T cells isolated from the decidua basalis and parietalis, umbilical cord blood, and maternal peripheral blood obtained from women who delivered a male neonate. As expected, T cells isolated from umbilical cord blood displayed a high *SRY/AR* ratio indicative of an exclusively fetal origin (Fig. 2D). In contrast, T cells isolated from the decidua parietalis and maternal peripheral blood had a *SRY/AR* ratio of zero, indicating that these cells are exclusively of maternal origin (Fig. 2D). T cells isolated from the decidua basalis were also predominantly of maternal origin (Fig. 2D).

Together, these findings indicate that both CD4+ and CD8+ maternal T cells exhibit an effector memory phenotype and release pro-inflammatory mediators at the human maternal-fetal interface during spontaneous preterm labor. In other words, the human syndrome of preterm labor is characterized by an increase in maternal effector/activated T cells at the maternal-fetal interface.

In vivo T-cell activation induces preterm birth by inducing hypothermia, bradycardia and cervical dilation

Next, we investigated the mechanisms whereby effector/activated T cells could induce preterm labor and birth by using a murine model. *In vivo* T-cell activation is achieved by the administration of an αCD3 antibody which induces a cytokine-related syndrome leading to hypothermia (90–94); therefore, we used this strategy in pregnant mice. Dams injected with αCD3ε delivered preterm (Fig. 3A), as previously reported (72). In order to understand the pathophysiology of preterm birth induced by T-cell activation, we compared this model to two well-established models of preterm birth: lipopolysaccharide (LPS)-induced (74, 95) (Fig. 3B) and RU486-induced (75) (Fig. 3C). Given that pregnant women undergoing complications associated with inflammatory responses can develop fever and tachycardia (96, 97) [as opposed to mice which develop hypothermia and bradycardia (74, 98)], we first evaluated the body temperature and heart rate of dams prior to preterm birth. Both αCD3ε and LPS induced hypothermia in dams (Fig. 3D&E), which could be due to the fact that these models are accompanied by excess release of TNFα into the circulation (78, 93). However, RU486 did not cause such an effect (Fig. 3F). Only the administration of αCD3ε induced maternal bradycardia (Fig. 3G-I), which may be a consequence of the severe hypothermia (99).

A hallmark of preterm labor in humans (100) and mice (101) is cervical dilation; therefore, we then measured the cervical width prior to preterm birth. Consistently, all of the stimuli (αCD3ε, LPS, and RU486) induced cervical dilation indicating that the three models share this aspect of parturition (Fig. 3J-L).

In order to prove that αCD3ε induced T-cell activation at the maternal-fetal interface and myometrium, we determined the expression of the CD3 molecule in total T cells (102, 103), the expression of the activation markers CD25 (104), CD69 (105), CD44 (106), CD62L

(107), CTLA-4 (108), and PD-1 (109) by CD4+ and CD8+ T cells, and the expression of IL2 by CD4+ T cells (103) and IFNγ by CD8+ T cells (110), in the decidua and myometrium (Fig. 4A). In line with our hypothesis (72), αCD3ε induced the downregulation of the CD3 molecule (Fig. 4B) and increased the expression of CD25 (Fig. 4C&D) and CD69 (Fig. 4E&F) by CD4+ and CD8+ T cells in both the decidua and myometrium. Upregulation of these activation markers was also observed in response to LPS (Fig. 4C-F), although the increased expression of CD25 in decidual T cells did not reach significance (Fig. 4C&D). In contrast, RU486 did not cause major changes in the expression of these activation markers by decidual and myometrial T cells (Fig. 4B-F). The expression of CD44 and CD62L was not drastically changed upon T-cell activation or treatment with LPS or RU486 (data not shown). Yet, the expression of CTLA-4 and PD-1 was variably regulated by CD4+ T cells and CD8+ T cells upon T-cell activation in the decidua and/or myometrium, but not upon treatment with LPS or RU486 (data not shown).

Injection with αCD3ε upregulated the expression of IL2 by CD4+ T cells in the decidua and myometrium (Fig. 4G). However, injection with αCD3ε increased the proportion of CD8+IFNγ+ T cells in the myometrium, but not in the decidua (Fig. 4H). These data suggest that, upon T-cell activation, T-cell responses are differentially regulated at the maternal-fetal interface and in the reproductive tissues. We also observed that LPS increased the infiltration of decidual CD8+ T cells expressing IFNγ, which is considered to be a response to microbial products (111). CD8+ T cells expressing IFNγ in the RU486 model were rare and did not vary (Fig. 4H).

Administration of αCD3ε induced the downregulation of the CD3 molecule in the spleen but not in the ULN (Fig. S2A&B). Dams injected with αCD3ε displayed greater proportions of CD4+ and CD8+ T cells expressing CD25 and CD69, but these dams did not have more IL-2-expressing CD4+ T cells or IFNγ-expressing CD8+ T cells, in the spleen and ULN compared to controls (Fig. S2C-H). Dams injected with LPS also had higher proportions of CD4+ or CD8+ T cells expressing CD25 and CD69 in the spleen and ULN compared to controls, but no changes in IL-2-expressing CD4+ T cells or IFNγ-expressing CD8+ T cells (Fig. S2C-H). Treatment with RU486 did not induce any changes in the expression of activation markers by splenic and ULN T cells (Fig. S2A-H). The expression of CD44, CD62L, CTLA-4, and PD-1 were variably regulated in the lymphatic tissues upon T-cell activation, but not drastically changed after treatment with LPS or RU486 (data not shown).

Collectively, these data show that αCD3ε causes preterm labor and birth by activating T cells at the maternal-fetal interface, myometrium, and systemically; yet, decidual and myometrial T-cell responses are distinct from those observed in lymphatic tissues. Such T-cell activation induces pathophysiological processes, some of which are shared with the microbial-inflammation (LPS) model but are distinct from the progesterone-dependent (RU486) model.

Given the association between regulatory T cells and pregnancy success (42, 50), we also evaluated whether αCD3ε could induce a reduction of such cells. Anti-CD3ε did not reduce the proportion of CD4+ regulatory T cells at the maternal-fetal interface, myometrium, or the maternal circulation (data not shown).

In vivo T-cell activation induces B-cell cytokine responses and pro-inflammatory macrophage polarization but does not lead to an increased neutrophil influx into the maternal-fetal interface and myometrium

Activation of T cells is accompanied by B-cell cytokine responses (112). Thus, we determined whether prior to preterm birth, αCD3ε could trigger B-cell activation at the maternal-fetal interface and myometrium (Fig. 4I). Anti-CD3ε caused an increase in the proportion of B cells expressing IFNγ in the decidua and myometrium (Fig. 4J). LPS also induced an increment in the proportion of activated B cells in the decidua but such an effect was not observed with RU486 (Fig. 4J). B cells expressing IFNγ in the RU486 model were rare (Fig. 4J).

Activation of T cells can also induce macrophage polarization (113, 114). Indeed, an M1-like (i.e. pro-inflammatory) macrophage polarization has been implicated in the mechanisms that lead to spontaneous preterm labor and birth (33). Hence, we evaluated whether prior to preterm birth, αCD3ε could induce macrophage activation and polarization towards M1-like and M2-like phenotypes at the maternal-fetal interface. First, flow cytometry was performed to identify M1-like (CD11b+F4/80+iNOS+ cells) and M2-like (CD11b+F4/80Arg1+IL10+ cells) macrophages in the decidua and myometrium. Anti-CD3ε increased the proportion of M1-like macrophages in the decidua and myometrium (Fig. 5A). However, neither LPS nor RU486 altered the proportion of M1-like macrophages at the maternal-fetal interface or the myometrium (data not shown). Although M2-like macrophages were detected at the maternal-fetal interface and myometrium, their proportions were unchanged upon αCD3ε, LPS, or RU486 injection (data not shown). In order to confirm that T-cell activation induced the polarization of M1-like macrophages, we determined the mRNA expression of multiple established M1 and M2 macrophage markers (115) in sorted decidual and myometrial macrophages (Fig. 5B). Anti-CD3ε caused a strong upregulation of M1 markers in macrophages from both the decidua and myometrium (Fig. 5C). LPS also induced an increase in the expression of M1 markers in the decidual macrophages, yet this effect was minimal in myometrial macrophages (Fig. 5C). However, RU486 did not dramatically affect the expression of M1 markers by decidual or myometrial macrophages (Fig. 5C). Furthermore, we found that αCD3ε induced the upregulation of some M2 markers by decidual and myometrial macrophages (Fig. 5D). LPS had a similar effect, but RU486 did not drastically affect the expression of M2 macrophage markers in the decidua and myometrium (Fig. 5D). Together, these results show that T-cell activation induces the polarization of M1 and M2 macrophages in the decidua and myometrium, yet favors their pro-inflammatory phenotype at the maternal-fetal interface.

Neutrophils are central players in the acute innate immune responses related to preterm labor associated with intra-amniotic inflammation/infection (116–121). Indeed, an influx of neutrophils in the decidua and myometrium is observed prior to LPS-induced preterm labor/birth (32, 122). Consistently, we showed that LPS caused increased neutrophil infiltration in the decidua and myometrium (Fig. 5E). However, such a neutrophilic response was not observed upon αCD3ε or RU486 injection (Fig. 5E). These data are relevant since they suggest that *in vivo* T-cell activation induces preterm labor in the absence of an augmented

neutrophil infiltration at the maternal-fetal interface and myometrium, indicating that it is a distinct inflammatory process from that induced by bacteria.

Taken together, these data demonstrate that *in vivo* T-cell activation induces preterm labor and birth by initiating B-cell cytokine responses and inducing macrophage pro-inflammatory polarization; yet, these inflammatory responses are independent of an increased neutrophil infiltration at the maternal-fetal interface and myometrium.

In vivo T-cell activation induces local and systemic maternal pro-inflammatory responses and the contractility pathway prior to preterm birth

Preterm labor is characterized by the upregulation of inflammatory mediators in the decidua (34, 123–126), myometrium (34, 127–129), and cervix (130). Such inflammatory mediators include cytokines (34, 126), chemokines (126, 131, 132), adhesion molecules (133, 134), and inflammasome components (135, 136). Quantitative RT-PCR profiling revealed that both αCD3ε and LPS caused the upregulation of several inflammatory mediators in the decidua and myometrium (Fig. 6A&B). However, there were subtle differences between the genes upregulated by αCD3ε and LPS (Fig. 6C&D). For example, whereas chemokines (*Ccl2*, *Ccl5*, *Ccl17*, *Ccl22*, *Cxcl9*, and *Cxcl10*), cytokines (*Il6* and *Ifng*), T-cell activation molecules (*Ctla4*, *Pdcd1* and *Sell*) and inflammasome components (*Pycard*, *Nod1*, and *Casp1*) were upregulated in both the αCD3ε and LPS models, *Il1b* was only upregulated in the LPS model in the decidual tissues (Fig. 6C). In the myometrial tissues, both αCD3ε and LPS caused the upregulation of *Ccl2*, *Ccl5*, *Ccl17*, *Ccl22*, *Cxcl9*, *Cxcl10*, *Ifng*, *Pdcd1*, *Nod1*, and *Casp-1* but only LPS induced the upregulation of *Il6* (Fig. 6D). Most of the inflammatory genes in the decidua and myometrium were unchanged upon RU486 injection (Fig. 6C&D), confirming that this is a non-inflammatory model of preterm birth (137).

A systemic inflammatory response is associated with preterm labor in the context of clinical chorioamnionitis (138, 139) and acute pyelonephritis (140, 141). Hence, systemic inflammatory responses were determined by measuring inflammatory mediators in the maternal serum from each of the preterm birth models. Anti-CD3ε and LPS induced a systemic maternal inflammatory response as evidenced by the upregulation of IL6, IL18, IL17A, IL4, IL5, CCL5, CXCL10, G-CSF, and IFNγ in the maternal serum (Fig. S3). However, RU486 did not induce such an effect (Fig. S3).

A hallmark of preterm labor is the presence of myometrial contractions that result from the harmonious induction of uterine activation proteins such as prostaglandins and connexin-43 (142). We therefore determined whether the administration of αCD3ε upregulated the expression of contractility-related genes in the decidua and myometrium. An upregulation of contractility-related genes was observed upon injection of αCD3ε, LPS, and RU486 in both the decidua and myometrium (Fig. 6A&B). Yet, this upregulation was more similar between the αCD3ε and LPS stimuli. These results indicate that in all three models of preterm birth the common pathway of parturition takes place.

These findings show that *in vivo* T-cell activation induces local and systemic maternal pro-inflammatory responses which coincide with activation of the contractility pathway prior to preterm birth, resembling those observed in the microbial inflammation model.

In vivo T-cell activation induces intra-amniotic inflammation and impacts fetal growth prior to preterm birth

It is well documented that preterm labor, either in the context of infection or sterile inflammation (12, 143, 144), is accompanied by increased amniotic fluid concentrations of pro-inflammatory cytokines and chemokines (145). We therefore evaluated cytokine and chemokine concentrations in amniotic fluid prior to preterm birth. Anti-CD3ε induced a massive pro-inflammatory response in the amniotic cavity, which was even more severe than that generated by LPS (Fig. 7). For example, αCD3ε but not LPS induced the upregulation of IL9, IL10, IL17A, IL23, and IL28 (Fig. 7). Yet, both αCD3ε and LPS caused the upregulation of IL6, CCL3, CCL5, CXCL5, and G-CSF (Fig. 7). RU486-induced preterm labor/birth, however, occurred in the absence of elevated amniotic fluid cytokines, except for IL-23 (Fig. 7). These data indicate that *in vivo* T-cell activation induces an intra-amniotic inflammatory response, which is stronger than that induced by a microbial product.

Increased concentrations of amniotic fluid cytokines and chemokines are associated with fetal damage (146–149), indicating that inflammation can negatively impact the offspring (150, 151), namely fetal growth restriction (152). Thus, we followed up our amniotic fluid cytokine determinations with the evaluation of fetal growth parameters. Fetuses born to dams injected with αCD3ε and LPS were smaller and leaner than their respective controls, but no differences were found in the RU486 group (Fig. 8A&B). We also examined the appearance of the fetal lungs since intra-amniotic pro-inflammatory responses can cause fetal lung damage (153, 154) (Fig. 8C). In the three preterm birth models, the fetal lungs appeared different than those of controls (Fig. 8C). To complement these observations, we performed histological evaluation of the preterm and term neonatal lungs. Consistent with what is reported in humans (155), lungs from preterm neonates appeared morphologically immature (i.e. canalicular stage (156)) compared to those from term neonates (i.e. terminal sac stage (156)) (Fig. 8D). No evident differences in the architecture of the preterm neonatal lungs were observed between preterm birth models (data not shown).

As a whole, these findings show that *in vivo* T-cell activation induces an intra-amniotic pro-inflammatory response that can negatively impact the fetus, causing fetal growth restriction prior to preterm birth which is similar to what occurs in fetuses exposed to microbial products and extends into the neonatal period. Therefore, finding a strategy to treat the adverse effects of maternal T-cell activation during pregnancy was the next logical step.

In vivo T-cell activation-induced preterm labor and birth is prevented by treatment with progesterone

Parturition in animals (157), and likely in humans (158), is associated with a functional progesterone (P4) withdrawal. Thus, the administration of this steroid hormone is clinically used to prevent preterm birth (159–167). Therefore, we tested whether *in vivo* T-cell activation could induce a systemic withdrawal of P4 and whether its administration could prevent preterm labor/birth. Anti-CD3ε induced a drop in the systemic concentration of P4 (Fig. 9A). Thus, dams received P4 prior to T-cell activation, as shown in the treatment diagram (Fig. 9B). Strikingly, T-cell activation-induced preterm labor/birth was entirely prevented by treatment with P4, which was translated to a longer gestational length (Fig.

9C&D). Importantly, neonates born to dams injected with αCD3ε and treated with P4 had reduced mortality at birth compared to those injected with αCD3ε and the vehicle (sesame oil or SO) (Fig. 9E). Representative images showed that neonates born to dams injected with αCD3ε and treated with P4 are comparable in size to controls (SO + isotype and P4 + isotype) (Fig. 9F). Indeed, neonates born to dams injected with αCD3ε and treated with P4 thrived as indicated by the presence of the milk band which was not observed in those pups born to untreated dams who died shortly after delivery (Fig. 9G, rectangles).

It is well established that progesterone prevents preterm birth by exhibiting anti-inflammatory effects at the maternal-fetal interface, myometrium, and the cervix (168–170). Therefore, we next evaluated the global anti-inflammatory effect of progesterone in dams injected with αCD3ε. Targeted qRT-PCR profiling showed that, compared to control mice (SO+Isotype), treatment with P4 downregulated the expression of several inflammatory mediators induced by αCD3ε in the decidua and cervix, but such an effect was not as strong in the myometrium (Fig. 10A-C). For example, dams treated with P4 + αCD3ε had reduced expression of *Casp11*, *Ccl22*, *Icam1, Ctla4, Nod1,* and *Ccl5* in the decidua compared to dams injected with SO + αCD3ε (Fig. 10D). In the myometrium, only *Il33* was downregulated upon P4 + αCD3ε treatment (Fig. 10B). In addition, dams treated with P4 + αCD3ε had reduced expression of *Il33*, *Il6*, *Il12b, Il1a*, *Pycard*, and *Il4* in the cervical tissues compared to those injected with SO + αCD3ε (Fig. 10E).

Collectively, these findings provide further evidence that progesterone attenuates local inflammatory responses at the maternal-fetal interface and in the cervix, preventing T-cell activation-induced preterm labor and birth, which translates to reduced adverse neonatal outcomes.

DISCUSSION

The study herein presents evidence that effector/activated maternal T cells lead to pathological inflammation and subsequently preterm labor and birth. Specifically, we showed that effector memory and activated maternal T cells expressing granzyme B and perforin are enriched at the maternal-fetal interface of women with spontaneous preterm labor and birth. Next, using a murine model, we reported that prior to inducing preterm birth, *in vivo* T-cell activation causes maternal hypothermia, bradycardia, systemic inflammation, and cervical dilation, all of which are clinical signs associated with preterm labor. We also found that prior to preterm birth, *in vivo* T-cell activation induces B-cell cytokine responses, a pro-inflammatory macrophage polarization, and the upregulation of inflammatory mediators at the maternal-fetal interface and myometrium, in the absence of an increased influx of neutrophils. Moreover, we showed that *in vivo* T-cell activation triggers an intra-amniotic inflammatory response and causes fetal growth restriction prior to preterm birth. Lastly, we provided evidence that treatment with progesterone could serve as an anti-inflammatory strategy to prevent preterm birth and adverse neonatal outcomes induced by T-cell activation (Fig. 11).

We and others have shown that effector memory and/or activated T cells can be recruited by (57, 171), and are present at (58, 59, 172–179), the human maternal-fetal interface in term

pregnancy. However, providing a role for these T cells in the pathogenesis of pregnancy complications has been challenging because of the absence of the disease (e.g. preterm labor). Herein, we report that effector memory maternal T cells are enriched in the decidual tissues of women with spontaneous preterm labor, who delivered preterm. Such an increase was not observed in patients who underwent the physiological process of labor at term, indicating that these effector cells contribute solely to the pathological process of premature labor. Such T-cell responses could be antigen-dependent or antigen-independent; the latter could be driven by cytokines (85, 180). The conventional belief is that effector memory T cells recognized placental-fetal antigens (47, 50, 178, 181); yet, we suggest that both antigen-dependent and antigen-independent processes may occur at the human maternal-fetal interface during spontaneous preterm labor. In line with this concept, CD8+ T_{EMRA} cells, lymphocytes with high cytolytic activity in the absence of *in vitro* pre-stimulation and that can proliferate in an antigen-independent manner (84, 182), were more abundant in the decidual tissues of women with spontaneous preterm labor compared to those who delivered preterm in the absence of labor.

Effector CD4+ and CD8+ T cells express high levels of granzyme B and perforin, which are stored in cytolytic granules and upon activation are released towards the target cell (183–186). Recently, it was shown that term-isolated decidual CD8+ T cells can degranulate, proliferate and produce inflammatory mediators upon *in vitro* stimulation (179), suggesting a role for these cells in pregnancy complications. Herein, we show that both decidual CD4+ and CD8+ T cells can express increased levels of granzyme B and perforin in women with spontaneous preterm labor, providing conclusive evidence that decidual T cells exhibit an effector and pro-inflammatory phenotype during the pathological process of premature parturition.

To investigate the mechanisms whereby effector T cells lead to spontaneous preterm labor, we used a murine model of transient *in vivo* T-cell activation - the injection of the hamster αCD3 monoclonal antibody (72, 187). *In vivo* T-cell activation at the maternal-fetal interface and myometrium was proven by the downregulation of the CD3 molecule (188–190), the upregulation of activation markers (e.g. CD25 (104), CD69 (105), CTLA-4 (108), PD-1 (109)) in CD4+ and CD8+ T cells, and increased proportions of CD4+ T cells expressing IL-2 (191). *In vivo* T-cell activation also induced an increase in the proportion of IFNγ-expressing CD8+ T cells in the myometrium but not in the decidua. This is consistent with *in vitro* studies showing that CD3 stimulation triggers the expression of IFNγ by CD8+ T cells (110). IFNγ-expressing CD8+ T cells were also increased upon LPS injection in the decidua but not in the myometrium, suggesting that T cells respond differently in each anatomical compartment. The abundance of IFNγ-expressing CD8+ T cells in the myometrium, but not in the decidua, could be explained by the fact that this cytokine is implicated in myometrial function, including contractility (192, 193). Moreover, *in vivo* T-cell activation tended to increase the proportion of IFNγ-expressing B cells in the decidua and myometrium, resembling type 1 B-cell responses (112), indicating that CD3 stimulation induces preterm birth by boosting both T-cell and B-cell responses at the maternal-fetal interface and myometrium.

In vivo T-cell activation induced hypothermia and bradycardia prior to preterm birth. These conditions were likely due to the cytokine storm and lymphatic T-cell activation induced by the injection with αCD3ε (92, 187). Such systemic responses also occurred in mice injected with LPS, resembling a stage of endotoxemia (74, 78, 98). In contrast, dams injected with the progestin antagonist (RU486) did not present hypothermia or bradycardia, consistent with the absence of a systemic cytokine response. Yet, cervical dilation and upregulation of contractility-related genes in decidual and myometrial tissues was observed upon injection of αCD3ε, LPS, and RU486, indicating that *in vivo* T-cell activation triggers the common pathway of parturition. These data show that the *in vivo* activation of T cells induces preterm labor and birth by initiating systemic and local pathophysiological processes, which partially resemble those induced by microbial products but are different from those caused by the blockage of progesterone action.

In vivo T-cell activation also had unique effects on innate immune cells at the maternal-fetal interface and myometrium. Previous studies have shown that macrophage activation is complex and does not tally with the M1/M2 polarization model (194). Similarly, at the human maternal-fetal interface, macrophage phenotypes do not entirely fit the M1/M2 polarization model (195, 196); yet, these cells possess a pro-inflammatory phenotype (M1-like) in women who underwent spontaneous preterm labor (33). Consistently, we found that, prior to *in vivo* T-cell activation-induced preterm birth, a predominantly pro-inflammatory (M1-like) macrophage polarization was observed at the murine maternal-fetal interface and myometrium. In this context, a pro-inflammatory macrophage polarization could have been driven by cytokines released upon T-cell activation (197). Importantly, *in vivo* T-cell activation did not cause an increase in the infiltration of neutrophils in the decidua and myometrium prior to preterm birth. Such an increase in neutrophils has been consistently observed in the context of preterm labor/birth associated with intra-amniotic infection (32, 122, 198–200) but not in the anti-progestin model (198, 199). Thus, we surmise that *in vivo* T-cell activation induces preterm birth by initiating immune responses that are partially different from those triggered by microbes and distinct from those caused by anti-progestins. In addition, these results indicate that the model of *in vivo* T-cell activation-induced preterm birth occurs in the absence of neutrophilic infiltration, which is distinct from the most commonly studied cause of preterm labor/birth, intra-amniotic infection (8, 201, 202).

Yet, *in vivo* T-cell activation-induced preterm labor/birth was accompanied by the upregulation of inflammatory mediators at the maternal-fetal interface and myometrium as well as in the maternal circulation and amniotic cavity. These local (10, 124, 125, 139, 145, 203) and systemic (204–206) immune responses have been frequently observed in women who undergo spontaneous preterm labor with intra-amniotic infection and/or inflammation. Therefore, the *in vivo* T-cell activation-induced preterm labor/birth model shares the local and systemic inflammatory responses with the microbial-induced preterm labor/birth model. The severe inflammatory responses in the amniotic cavity explained the deleterious effect observed in fetuses (fetal growth restriction) born to dams injected with αCD3 and LPS. In contrast, the RU486-induced preterm labor/birth model is characterized by the absence of local and systemic inflammation, but the fetal lungs are hemorrhagic that could be due to the adverse effects of this anti-progestin (207).

In vivo T-cell activation-induced preterm labor/birth was prevented by treatment with progesterone. Importantly, the adverse neonatal outcomes induced upon T-cell activation were also ameliorated. Indeed, most of the neonates born to dams injected with αCD3 and treated with progesterone thrived. The protective effects of progesterone during pregnancy have been previously shown to be mediated, at least in part, by modulating T-cell responses (208–210). Indeed, we have previously shown that progesterone prevents endotoxin-induced preterm birth by fostering an anti-inflammatory response at the maternal-fetal interface, characterized by fewer effector T cells, activated macrophages, and neutrophils, as well as increased regulatory T cells (168). The anti-inflammatory effects of progesterone were reflected in the cervical tissues as well (168). Progesterone also has anti-inflammatory effects in the systemic circulation and myometrium (168, 170). Herein, we provide further evidence of the anti-inflammatory effects of progesterone. Specifically, we show that progesterone attenuated the local pro-inflammatory responses at the maternal-fetal interface and the cervix. Of interest, progesterone dampened genes related to the inflammasome pathway (e.g. *Casp11*, *Pycard*, *Nod1*), which has been strongly associated with the mechanisms initiating the pathological process of preterm labor (20, 135, 136, 211–214). Collectively, these results demonstrate that preterm labor/birth and adverse neonatal outcomes induced by T-cell activation can be treated by using the anti-inflammatory effects of progesterone, a clinically approved therapy.

It is worth mentioning that, following T-cell activation, progesterone did not strongly impact the expression of inflammatory genes in the myometrium, except for upregulating the expression of *Il33*. The expression of this cytokine, however, was attenuated in the cervix, indicating that each anatomical compartment is differentially regulated by progesterone. This concept is in line with our initial findings indicating that T-cell activation and LPS trigger different responses in the decidua and myometrium. This last observation provides an example of the complexity of immune interactions at the maternal-fetal interface and in the reproductive tissues: each compartment must regulate specific mediators which contribute to the complex phenomenon of parturition.

A central question that remains unanswered is what causes T-cell activation leading to spontaneous preterm labor and birth in women. The most tempting explanation is that placental-fetal antigens induce the activation of maternal T cells in the systemic circulation and/or at the maternal-fetal interface. These antigens could have been presented by APCs in the spleen and uterine-draining lymph nodes and/or at the maternal-fetal interface (67, 215). However, such a hypothesis is difficult to prove in humans (67). A second possibility is that effector memory T cells are not specific for placental-fetal antigens, but instead they recognize microbe-derived peptides which are normally present in the basal plate of the placenta (216) and/or the endometrium (217). Such T cells can then proliferate in an antigen-independent manner by pro-inflammatory mediators (180) induced by dangers signals or alarmins in the intra-amniotic space (i.e. sterile intra-amniotic inflammation) (145). This concept is supported by the fact that most cases of preterm labor take place in the setting of sterile intra-amniotic inflammation (12, 143), which can occur in the absence of acute histologic chorioamnionitis [neutrophil infiltration in the chorioamniotic membranes (218)] (143, 219). A third possibility is that effector memory T cells at the maternal-fetal interface are virus-specific; however, a clear association between viral infections and human

preterm labor requires further epidemiological studies. In this latter context, it has been suggested that maternal-fetal tolerance is compromised by the virus and polymicrobial infections can take place, inducing preterm labor and birth (21, 220–222). Further research is required to investigate the antigen specificity and clonality of effector memory T cells at the maternal-fetal interface in the context of preterm labor and birth.

Supplementary Material

Refer to Web version on PubMed Central for supplementary material.

ACKNOWLEDGMENTS

We thank the physicians, nurses, and research assistants from the Center for Advanced Obstetrical Care and Research, Intrapartum Unit, PRB Clinical Laboratory, and PRB Perinatal Translational Science Laboratory for their help with collecting and processing samples. We also thank George Schwenkel, Yaozhu Leng, Hong Meng, Ronald Unkel, Ryan Cantarella, Pablo Silva, Chengrui Zou, Jennifer Pierluissi, and Yang Jiang, for their help with carrying out some of the experiments and/or crucial reading of the manuscript.

REFERENCES

1. Blencowe H, Cousens S, Oestergaard MZ, Chou D, Moller AB, Narwal R, Adler A, Vera Garcia C, Rohde S, Say L, and Lawn JE. 2012 National, regional, and worldwide estimates of preterm birth rates in the year 2010 with time trends since 1990 for selected countries: a systematic analysis and implications. Lancet 379: 2162–2172. [PubMed: 22682464]
2. Liu L, Oza S, Hogan D, Perin J, Rudan I, Lawn JE, Cousens S, Mathers C, and Black RE. 2015 Global, regional, and national causes of child mortality in 2000–13, with projections to inform post-2015 priorities: an updated systematic analysis. Lancet 385: 430–440. [PubMed: 25280870]
3. Goldenberg RL, Culhane JF, Iams JD, and Romero R. 2008 Epidemiology and causes of preterm birth. Lancet 371: 75–84. [PubMed: 18177778]
4. Romero R, and Lockwood CJ. 2009 Pathogenesis of Spontaneous Preterm Labor In Creasy and Resnik's Maternal-Fetal Medicine: Principles and Practice, Sixth ed. Creasy RK, Resnik R, and Iams J, eds. Elsevier, Philadelphia 521–543.
5. Muglia LJ, and Katz M. 2010 The enigma of spontaneous preterm birth. N Engl J Med 362: 529–535. [PubMed: 20147718]
6. Romero R, Dey SK, and Fisher SJ. 2014 Preterm labor: one syndrome, many causes. Science 345: 760–765. [PubMed: 25124429]
7. Barros FC, Papageorghiou AT, Victora CG, Noble JA, Pang R, Iams J, Cheikh Ismail L, Goldenberg RL, Lambert A, Kramer MS, Carvalho M, Conde-Agudelo A, Jaffer YA, Bertino E, Gravett MG, Altman DG, Ohuma EO, Purwar M, Frederick IO, Bhutta ZA, Kennedy SH, Villar J, International F, and Newborn C Growth Consortium for the 21st. 2015 The distribution of clinical phenotypes of preterm birth syndrome: implications for prevention. JAMA Pediatr 169: 220–229. [PubMed: 25561016]
8. Romero R, Mazor M, Wu YK, Sirtori M, Oyarzun E, Mitchell MD, and Hobbins JC. 1988 Infection in the pathogenesis of preterm labor. Semin Perinatol 12: 262–279. [PubMed: 3065940]
9. Gravett MG, Witkin SS, Haluska GJ, Edwards JL, Cook MJ, and Novy MJ. 1994 An experimental model for intraamniotic infection and preterm labor in rhesus monkeys. Am J Obstet Gynecol 171: 1660–1667. [PubMed: 7802084]
10. Yoon BH, Romero R, Moon JB, Shim SS, Kim M, Kim G, and Jun JK. 2001 Clinical significance of intra-amniotic inflammation in patients with preterm labor and intact membranes. Am J Obstet Gynecol 185: 1130–1136. [PubMed: 11717646]
11. Whidbey C, Harrell MI, Burnside K, Ngo L, Becraft AK, Iyer LM, Aravind L, Hitti J, Adams Waldorf KM, and Rajagopal L. 2013 A hemolytic pigment of Group B Streptococcus allows bacterial penetration of human placenta. J Exp Med 210: 1265–1281. [PubMed: 23712433]

12. Combs CA, Gravett M, Garite TJ, Hickok DE, Lapidus J, Porreco R, Rael J, Grove T, Morgan TK, Clewell W, Miller H, Luthy D, Pereira L, Nageotte M, Robilio PA, Fortunato S, Simhan H, Baxter JK, Amon E, Franco A, Trofatter K, and Heyborne K. 2014 Amniotic fluid infection, inflammation, and colonization in preterm labor with intact membranes. Am J Obstet Gynecol 210: 125.e121–125.e115. [PubMed: 24274987]
13. Janeway CA Jr. 1989 Approaching the asymptote? Evolution and revolution in immunology. Cold Spring Harb Symp Quant Biol 54 Pt 1: 1–13.
14. Matzinger P 1998 An innate sense of danger. Semin Immunol 10: 399–415. [PubMed: 9840976]
15. Oppenheim JJ, and Yang D. 2005 Alarmins: chemotactic activators of immune responses. Curr Opin Immunol 17: 359–365. [PubMed: 15955682]
16. Lotze MT, Deisseroth A, and Rubartelli A. 2007 Damage associated molecular pattern molecules. Clin Immunol 124: 1–4. [PubMed: 17468050]
17. Takeuchi O, and Akira S. 2010 Pattern recognition receptors and inflammation. Cell 140: 805–820. [PubMed: 20303872]
18. Kim YM, Romero R, Chaiworapongsa T, Kim GJ, Kim MR, Kuivaniemi H, Tromp G, Espinoza J, Bujold E, Abrahams VM, and Mor G. 2004 Toll-like receptor-2 and −4 in the chorioamniotic membranes in spontaneous labor at term and in preterm parturition that are associated with chorioamnionitis. Am J Obstet Gynecol 191: 1346–1355. [PubMed: 15507964]
19. Mittal P, Romero R, Kusanovic JP, Edwin SS, Gotsch F, Mazaki-Tovi S, Espinoza J, Erez O, Nhan-Chang CL, Than NG, Vaisbuch E, and Hassan SS. 2008 CXCL6 (granulocyte chemotactic protein-2): a novel chemokine involved in the innate immune response of the amniotic cavity. Am J Reprod Immunol 60: 246–257. [PubMed: 18782286]
20. Gotsch F, Romero R, Chaiworapongsa T, Erez O, Vaisbuch E, Espinoza J, Kusanovic JP, Mittal P, Mazaki-Tovi S, Kim CJ, Kim JS, Edwin S, Nhan-Chang CL, Hamill N, Friel L, Than NG, Mazor M, Yoon BH, and Hassan SS. 2008 Evidence of the involvement of caspase-1 under physiologic and pathologic cellular stress during human pregnancy: a link between the inflammasome and parturition. J Matern Fetal Neonatal Med 21: 605–616. [PubMed: 18828051]
21. Cardenas I, Means RE, Aldo P, Koga K, Lang SM, Booth CJ, Manzur A, Oyarzun E, Romero R, and Mor G. 2010 Viral infection of the placenta leads to fetal inflammation and sensitization to bacterial products predisposing to preterm labor. J Immunol 185: 1248–1257. [PubMed: 20554966]
22. Ilievski V, and Hirsch E. 2010 Synergy between viral and bacterial toll-like receptors leads to amplification of inflammatory responses and preterm labor in the mouse. Biol Reprod 83: 767–773. [PubMed: 20650880]
23. Abrahams VM 2011 The role of the Nod-like receptor family in trophoblast innate immune responses. J Reprod Immunol 88: 112–117. [PubMed: 21277024]
24. Romero R, Chaiworapongsa T, Alpay Savasan Z, Xu Y, Hussein Y, Dong Z, Kusanovic JP, Kim CJ, and Hassan SS. 2011 Damage-associated molecular patterns (DAMPs) in preterm labor with intact membranes and preterm PROM: a study of the alarmin HMGB1. J Matern Fetal Neonatal Med 24: 1444–1455. [PubMed: 21958433]
25. Lappas M 2013 NOD1 and NOD2 regulate proinflammatory and prolabor mediators in human fetal membranes and myometrium via nuclear factor-kappa B. Biol Reprod 89: 14. [PubMed: 23740944]
26. Jaiswal MK, Agrawal V, Mallers T, Gilman-Sachs A, Hirsch E, and Beaman KD. 2013 Regulation of apoptosis and innate immune stimuli in inflammation-induced preterm labor. J Immunol 191: 5702–5713. [PubMed: 24163412]
27. Koga K, Izumi G, Mor G, Fujii T, and Osuga Y. 2014 Toll-like receptors at the maternal-fetal interface in normal pregnancy and pregnancy complications. Am J Reprod Immunol 72: 192–205. [PubMed: 24754320]
28. Agrawal V, Jaiswal MK, Ilievski V, Beaman KD, Jilling T, and Hirsch E. 2014 Platelet-activating factor: a role in preterm delivery and an essential interaction with Toll-like receptor signaling in mice. Biol Reprod 91: 119. [PubMed: 25253732]

29. Negishi Y, Shima Y, Takeshita T, and Takahashi H. 2017 Distribution of invariant natural killer T cells and dendritic cells in late pre-term birth without acute chorioamnionitis. Am J Reprod Immunol 77.
30. Musilova I, Andrys C, Krejsek J, Drahosova M, Zednikova B, Pliskova L, Zemlickova H, Jacobsson B, and Kacerovsky M. 2017 Amniotic fluid pentraxins: Potential early markers for identifying intra-amniotic inflammatory complications in preterm pre-labor rupture of membranes. Am J Reprod Immunol.
31. Xu Y, Romero R, Miller D, Silva P, Panaitescu B, Theis KR, Arif A, Hassan SS, and Gomez-Lopez N. 2018 Innate lymphoid cells at the human maternal-fetal interface in spontaneous preterm labor. Am J Reprod Immunol 79: e12820. [PubMed: 29457302]
32. Arenas-Hernandez M, Romero R, St Louis D, Hassan SS, Kaye EB, and Gomez-Lopez N. 2016 An imbalance between innate and adaptive immune cells at the maternal-fetal interface occurs prior to endotoxin-induced preterm birth. Cell Mol Immunol 13: 462–473. [PubMed: 25849119]
33. Xu Y, Romero R, Miller D, Kadam L, Mial TN, Plazyo O, Garcia-Flores V, Hassan SS, Xu Z, Tarca AL, Drewlo S, and Gomez-Lopez N. 2016 An M1-like Macrophage Polarization in Decidual Tissue during Spontaneous Preterm Labor That Is Attenuated by Rosiglitazone Treatment. J Immunol 196: 2476–2491. [PubMed: 26889045]
34. St Louis D, Romero R, Plazyo O, Arenas-Hernandez M, Panaitescu B, Xu Y, Milovic T, Xu Z, Bhatti G, Mi QS, Drewlo S, Tarca AL, Hassan SS, and Gomez-Lopez N. 2016 Invariant NKT Cell Activation Induces Late Preterm Birth That Is Attenuated by Rosiglitazone. J Immunol 196: 1044–1059. [PubMed: 26740111]
35. Gomez-Lopez N, Romero R, Arenas-Hernandez M, Schwenkel G, St Louis D, Hassan SS, and Mial TN. 2017 In vivo activation of invariant natural killer T cells induces systemic and local alterations in T-cell subsets prior to preterm birth. Clin Exp Immunol 189: 211–225. [PubMed: 28369855]
36. Abbas AK, and Janeway CA Jr. 2000 Immunology: improving on nature in the twenty-first century. Cell 100: 129–138. [PubMed: 10647937]
37. Shima T, Sasaki Y, Itoh M, Nakashima A, Ishii N, Sugamura K, and Saito S. 2010 Regulatory T cells are necessary for implantation and maintenance of early pregnancy but not late pregnancy in allogeneic mice. J Reprod Immunol 85: 121–129. [PubMed: 20439117]
38. Moldenhauer LM, Keenihan SN, Hayball JD, and Robertson SA. 2010 GM-CSF is an essential regulator of T cell activation competence in uterine dendritic cells during early pregnancy in mice. J Immunol 185: 7085–7096. [PubMed: 20974989]
39. Chen T, Darrasse-Jeze G, Bergot AS, Courau T, Churlaud G, Valdivia K, Strominger JL, Ruocco MG, Chaouat G, and Klatzmann D. 2013 Self-specific memory regulatory T cells protect embryos at implantation in mice. J Immunol 191: 2273–2281. [PubMed: 23913969]
40. Heitmann RJ, Weitzel RP, Feng Y, Segars JH, Tisdale JF, and Wolff EF. 2017 Maternal T Regulatory Cell Depletion Impairs Embryo Implantation Which Can Be Corrected With Adoptive T Regulatory Cell Transfer. Reprod Sci 24: 1014–1024. [PubMed: 27834288]
41. Bonney EA 2001 Maternal tolerance is not critically dependent on interleukin-4. Immunology 103: 382–389. [PubMed: 11454068]
42. Aluvihare VR, Kallikourdis M, and Betz AG. 2004 Regulatory T cells mediate maternal tolerance to the fetus. Nat Immunol 5: 266–271. [PubMed: 14758358]
43. Somerset DA, Zheng Y, Kilby MD, Sansom DM, and Drayson MT. 2004 Normal human pregnancy is associated with an elevation in the immune suppressive CD25+ CD4+ regulatory T-cell subset. Immunology 112: 38–43. [PubMed: 15096182]
44. Heikkinen J, Mottonen M, Alanen A, and Lassila O. 2004 Phenotypic characterization of regulatory T cells in the human decidua. Clin Exp Immunol 136: 373–378. [PubMed: 15086404]
45. Sasaki Y, Sakai M, Miyazaki S, Higuma S, Shiozaki A, and Saito S. 2004 Decidual and peripheral blood CD4+CD25+ regulatory T cells in early pregnancy subjects and spontaneous abortion cases. Mol Hum Reprod 10: 347–353. [PubMed: 14997000]
46. Kahn DA, and Baltimore D. 2010 Pregnancy induces a fetal antigen-specific maternal T regulatory cell response that contributes to tolerance. Proc Natl Acad Sci U S A 107: 9299–9304. [PubMed: 20439708]

47. Bonney EA, Shepard MT, and Bizargity P. 2011 Transient modification within a pool of CD4 T cells in the maternal spleen. Immunology 134: 270–280. [PubMed: 21977997]

48. Ramhorst R, Fraccaroli L, Aldo P, Alvero AB, Cardenas I, Leiros CP, and Mor G. 2012 Modulation and recruitment of inducible regulatory T cells by first trimester trophoblast cells. Am J Reprod Immunol 67: 17–27. [PubMed: 21819477]

49. Samstein RM, Josefowicz SZ, Arvey A, Treuting PM, and Rudensky AY. 2012 Extrathymic generation of regulatory T cells in placental mammals mitigates maternal-fetal conflict. Cell 150: 29–38. [PubMed: 22770213]

50. Rowe JH, Ertelt JM, Xin L, and Way SS. 2012 Pregnancy imprints regulatory memory that sustains anergy to fetal antigen. Nature 490: 102–106. [PubMed: 23023128]

51. Erlebacher A 2013 Mechanisms of T cell tolerance towards the allogeneic fetus. Nat Rev Immunol 13: 23–33. [PubMed: 23237963]

52. La Rocca C, Carbone F, Longobardi S, and Matarese G. 2014 The immunology of pregnancy: regulatory T cells control maternal immune tolerance toward the fetus. Immunol Lett 162: 41–48. [PubMed: 24996040]

53. Wegorzewska M, Nijagal A, Wong CM, Le T, Lescano N, Tang Q, and MacKenzie TC. 2014 Fetal intervention increases maternal T cell awareness of the foreign conceptus and can lead to immune-mediated fetal demise. J Immunol 192: 1938–1945. [PubMed: 24415782]

54. Bonney EA, and Brown SA. 2014 To drive or be driven: the path of a mouse model of recurrent pregnancy loss. Reproduction 147: R153–167. [PubMed: 24472815]

55. Bonney EA 2017 Alternative theories: Pregnancy and immune tolerance. J Reprod Immunol 123: 65–71. [PubMed: 28941880]

56. Aghaeepour N, Ganio EA, McIlwain D, Tsai AS, Tingle M, Van Gassen S, Gaudilliere DK, Baca Q, McNeil L, Okada R, Ghaemi MS, Furman D, Wong RJ, Winn VD, Druzin ML, El-Sayed YY, Quaintance C, Gibbs R, Darmstadt GL, Shaw GM, Stevenson DK, Tibshirani R, Nolan GP, Lewis DB, Angst MS, and Gaudilliere B. 2017 An immune clock of human pregnancy. Sci Immunol 2.

57. Gomez-Lopez N, Estrada-Gutierrez G, Jimenez-Zamudio L, Vega-Sanchez R, and Vadillo-Ortega F. 2009 Fetal membranes exhibit selective leukocyte chemotaxic activity during human labor. J Reprod Immunol 80: 122–131. [PubMed: 19406481]

58. Gomez-Lopez N, Vadillo-Perez L, Hernandez-Carbajal A, Godines-Enriquez M, Olson DM, and Vadillo-Ortega F. 2011 Specific inflammatory microenvironments in the zones of the fetal membranes at term delivery. Am J Obstet Gynecol 205: 235 e215–224.

59. Gomez-Lopez N, Vega-Sanchez R, Castillo-Castrejon M, Romero R, Cubeiro-Arreola K, and Vadillo-Ortega F. 2013 Evidence for a role for the adaptive immune response in human term parturition. Am J Reprod Immunol 69: 212–230. [PubMed: 23347265]

60. Gomez-Lopez N, Olson DM, and Robertson SA. 2016 Interleukin-6 controls uterine Th9 cells and CD8(+) T regulatory cells to accelerate parturition in mice. Immunol Cell Biol 94: 79–89. [PubMed: 26073576]

61. Tarca AL, Romero R, Xu Z, Gomez-Lopez N, Erez O, Hsu C-D, Hassan SS, and Carey VJ. 2019 Targeted expression profiling by RNA-Seq improves detection of cellular dynamics during pregnancy and identifies a role for T cells in term parturition. Scientific Reports 9: 848. [PubMed: 30696862]

62. Kim CJ, Romero R, Kusanovic JP, Yoo W, Dong Z, Topping V, Gotsch F, Yoon BH, Chi JG, and Kim JS. 2010 The frequency, clinical significance, and pathological features of chronic chorioamnionitis: a lesion associated with spontaneous preterm birth. Mod Pathol 23: 1000–1011. [PubMed: 20348884]

63. Lee J, Kim JS, Park JW, Park CW, Park JS, Jun JK, and Yoon BH. 2013 Chronic chorioamnionitis is the most common placental lesion in late preterm birth. Placenta 34: 681–689. [PubMed: 23684379]

64. Kim CJ, Romero R, Chaemsaithong P, and Kim JS. 2015 Chronic inflammation of the placenta: definition, classification, pathogenesis, and clinical significance. Am J Obstet Gynecol 213: S53–69. [PubMed: 26428503]

65. Xu Y, Tarquini F, Romero R, Kim CJ, Tarca AL, Bhatti G, Lee J, Sundell IB, Mittal P, Kusanovic JP, Hassan SS, and Kim JS. 2012 Peripheral CD300a+CD8+ T lymphocytes with a distinct

cytotoxic molecular signature increase in pregnant women with chronic chorioamnionitis. Am J Reprod Immunol 67: 184–197. [PubMed: 22077960]

66. Nancy P, Tagliani E, Tay CS, Asp P, Levy DE, and Erlebacher A. 2012 Chemokine gene silencing in decidual stromal cells limits T cell access to the maternal-fetal interface. Science 336: 1317–1321. [PubMed: 22679098]
67. Nancy P, and Erlebacher A. 2014 T cell behavior at the maternal-fetal interface. Int J Dev Biol 58: 189–198. [PubMed: 25023685]
68. Nancy P, Siewiera J, Rizzuto G, Tagliani E, Osokine I, Manandhar P, Dolgalev I, Clementi C, Tsirigos A, and Erlebacher A. 2018 H3K27me3 dynamics dictate evolving uterine states in pregnancy and parturition. J Clin Invest 128: 233–247. [PubMed: 29202469]
69. Meuer SC, Hodgdon JC, Hussey RE, Protentis JP, Schlossman SF, and Reinherz EL. 1983 Antigen-like effects of monoclonal antibodies directed at receptors on human T cell clones. J Exp Med 158: 988–993. [PubMed: 6604129]
70. Leo O, Foo M, Sachs DH, Samelson LE, and Bluestone JA. 1987 Identification of a monoclonal antibody specific for a murine T3 polypeptide. Proc Natl Acad Sci U S A 84: 1374–1378. [PubMed: 2950524]
71. Ellenhorn JD, Schreiber H, and Bluestone JA. 1990 Mechanism of tumor rejection in anti-CD3 monoclonal antibody-treated mice. J Immunol 144: 2840–2846. [PubMed: 1969454]
72. Gomez-Lopez N, Romero R, Arenas-Hernandez M, Ahn H, Panaitescu B, Vadillo-Ortega F, Sanchez-Torres C, Salisbury KS, and Hassan SS. 2016 In vivo T-cell activation by a monoclonal alphaCD3epsilon antibody induces preterm labor and birth. Am J Reprod Immunol 76: 386–390. [PubMed: 27658719]
73. Xu Y, Plazyo O, Romero R, Hassan SS, and Gomez-Lopez N. 2015 Isolation of Leukocytes from the Human Maternal-fetal Interface. J Vis Exp: e52863. [PubMed: 26067211]
74. Gomez-Lopez N, Romero R, Arenas-Hernandez M, Panaitescu B, Garcia-Flores V, Mial TN, Sahi A, and Hassan SS. 2018 Intra-amniotic administration of lipopolysaccharide induces spontaneous preterm labor and birth in the absence of a body temperature change. J Matern Fetal Neonatal Med 31: 439–446. [PubMed: 28139962]
75. Dudley DJ, Branch DW, Edwin SS, and Mitchell MD. 1996 Induction of preterm birth in mice by RU486. Biol Reprod 55: 992–995. [PubMed: 8902208]
76. Gomez-Lopez N, Romero R, Plazyo O, Panaitescu B, Furcron AE, Miller D, Roumayah T, Flom E, and Hassan SS. 2016 Intra-Amniotic Administration of HMGB1 Induces Spontaneous Preterm Labor and Birth. Am J Reprod Immunol 75: 3–7. [PubMed: 26781934]
77. Furcron AE, Romero R, Mial TN, Balancio A, Panaitescu B, Hassan SS, Sahi A, Nord C, and Gomez-Lopez N. 2016 Human Chorionic Gonadotropin Has Anti-Inflammatory Effects at the Maternal-Fetal Interface and Prevents Endotoxin-Induced Preterm Birth, but Causes Dystocia and Fetal Compromise in Mice. Biol Reprod 94: 136. [PubMed: 27146032]
78. Garcia-Flores V, Romero R, Miller D, Xu Y, Done B, Veerapaneni C, Leng Y, Arenas-Hernandez M, Khan N, Panaitescu B, Hassan SS, Alvarez-Salas LM, and Gomez-Lopez N. 2018 Inflammation-Induced Adverse Pregnancy and Neonatal Outcomes Can Be Improved by the Immunomodulatory Peptide Exendin-4. Front Immunol 9: 1291. [PubMed: 29967606]
79. Arenas-Hernandez M, Sanchez-Rodriguez EN, Mial TN, Robertson SA, and Gomez-Lopez N. 2015 Isolation of Leukocytes from the Murine Tissues at the Maternal-Fetal Interface. J Vis Exp: e52866. [PubMed: 26067389]
80. Butcher EC, and Picker LJ. 1996 Lymphocyte homing and homeostasis. Science 272: 60–66. [PubMed: 8600538]
81. Garside P, Ingulli E, Merica RR, Johnson JG, Noelle RJ, and Jenkins MK. 1998 Visualization of specific B and T lymphocyte interactions in the lymph node. Science 281: 96–99. [PubMed: 9651253]
82. Ahmed R, and Gray D. 1996 Immunological memory and protective immunity: understanding their relation. Science 272: 54–60. [PubMed: 8600537]
83. Sallusto F, Lenig D, Forster R, Lipp M, and Lanzavecchia A. 1999 Two subsets of memory T lymphocytes with distinct homing potentials and effector functions. Nature 401: 708–712. [PubMed: 10537110]

84. Geginat J, Lanzavecchia A, and Sallusto F. 2003 Proliferation and differentiation potential of human CD8+ memory T-cell subsets in response to antigen or homeostatic cytokines. Blood 101: 4260–4266. [PubMed: 12576317]
85. Sallusto F, Geginat J, and Lanzavecchia A. 2004 Central memory and effector memory T cell subsets: function, generation, and maintenance. Annu Rev Immunol 22: 745–763. [PubMed: 15032595]
86. Wolint P, Betts MR, Koup RA, and Oxenius A. 2004 Immediate cytotoxicity but not degranulation distinguishes effector and memory subsets of CD8+ T cells. J Exp Med 199: 925–936. [PubMed: 15051762]
87. Grossman WJ, Verbsky JW, Tollefsen BL, Kemper C, Atkinson JP, and Ley TJ. 2004 Differential expression of granzymes A and B in human cytotoxic lymphocyte subsets and T regulatory cells. Blood 104: 2840–2848. [PubMed: 15238416]
88. Rock MT, Yoder SM, Wright PF, Talbot TR, Edwards KM, and Crowe JE Jr. 2005 Differential regulation of granzyme and perforin in effector and memory T cells following smallpox immunization. J Immunol 174: 3757–3764. [PubMed: 15749916]
89. Lin L, Couturier J, Yu X, Medina MA, Kozinetz CA, and Lewis DE. 2014 Granzyme B secretion by human memory CD4 T cells is less strictly regulated compared to memory CD8 T cells. BMC Immunol 15: 36. [PubMed: 25245659]
90. Hirsch R, Eckhaus M, Auchincloss H Jr., Sachs DH, and Bluestone JA. 1988 Effects of in vivo administration of anti-T3 monoclonal antibody on T cell function in mice. I. Immunosuppression of transplantation responses. J Immunol 140: 3766–3772. [PubMed: 3286764]
91. Hirsch R, Gress RE, Pluznik DH, Eckhaus M, and Bluestone JA. 1989 Effects of in vivo administration of anti-CD3 monoclonal antibody on T cell function in mice. II. In vivo activation of T cells. J Immunol 142: 737–743. [PubMed: 2521507]
92. Ferran C, Sheehan K, Dy M, Schreiber R, Merite S, Landais P, Noel LH, Grau G, Bluestone J, and Bach JF. 1990 Cytokine-related syndrome following injection of anti-CD3 monoclonal antibody: further evidence for transient in vivo T cell activation. Eur J Immunol 20: 509–515. [PubMed: 2138557]
93. Alegre M, Vandenabeele P, Flamand V, Moser M, Leo O, Abramowicz D, Urbain J, Fiers W, and Goldman M. 1990 Hypothermia and hypoglycemia induced by anti-CD3 monoclonal antibody in mice: role of tumor necrosis factor. Eur J Immunol 20: 707–710. [PubMed: 2138564]
94. Stankova J 1992 Anti-CD3 antibody-treated mice: in vivo induction of cytolytic activity and TNF production by lung leukocytes. Int J Cancer 51: 259–265. [PubMed: 1533202]
95. Fidel PL Jr., Romero R, Wolf N, Cutright J, Ramirez M, Araneda H, and Cotton DB. 1994 Systemic and local cytokine profiles in endotoxin-induced preterm parturition in mice. Am J Obstet Gynecol 170: 1467–1475. [PubMed: 8178889]
96. Galinsky R, Polglase GR, Hooper SB, Black MJ, and Moss TJ. 2013 The consequences of chorioamnionitis: preterm birth and effects on development. J Pregnancy 2013: 412831. [PubMed: 23533760]
97. Romero R, Chaemsaithong P, Korzeniewski SJ, Kusanovic JP, Docheva N, Martinez-Varea A, Ahmed AI, Yoon BH, Hassan SS, Chaiworapongsa T, and Yeo L. 2016 Clinical chorioamnionitis at term III: how well do clinical criteria perform in the identification of proven intra-amniotic infection? J Perinat Med 44: 23–32. [PubMed: 25918914]
98. Copeland S, Warren HS, Lowry SF, Calvano SE, and Remick D. 2005 Acute inflammatory response to endotoxin in mice and humans. Clinical and diagnostic laboratory immunology 12: 60–67. [PubMed: 15642986]
99. Mallet ML 2002 Pathophysiology of accidental hypothermia. QJM 95: 775–785. [PubMed: 12454320]
100. How HY, Khoury JC, and Sibai BM. 2009 Cervical dilatation on presentation for preterm labor and subsequent preterm birth. Am J Perinatol 26: 1–6. [PubMed: 19021099]
101. Mahendroo M 2018 Cervical hyaluronan biology in pregnancy, parturition and preterm birth. Matrix Biol.
102. Krangel MS 1987 Endocytosis and recycling of the T3-T cell receptor complex. The role of T3 phosphorylation. J Exp Med 165: 1141–1159. [PubMed: 3104527]

103. Neumann CM, Oughton JA, and Kerkvliet NI. 1992 Anti-CD3-induced T-cell activation in vivo--I. Flow cytometric analysis of dose-responsive, time-dependent, and cyclosporin A-sensitive parameters of CD4+ and CD8+ cells from the draining lymph nodes of C57Bl/6 mice. Int J Immunopharmacol 14: 1295–1304. [PubMed: 1452414]
104. Fazekas de St Groth B, Smith AL, and Higgins CA. 2004 T cell activation: in vivo veritas. Immunol Cell Biol 82: 260–268. [PubMed: 15186257]
105. Hara T, Jung LK, Bjorndahl JM, and Fu SM. 1986 Human T cell activation. III. Rapid induction of a phosphorylated 28 kD/32 kD disulfide-linked early activation antigen (EA 1) by 12-o-tetradecanoyl phorbol-13-acetate, mitogens, and antigens. J Exp Med 164: 1988–2005. [PubMed: 2946796]
106. Baaten BJ, Li CR, and Bradley LM. 2010 Multifaceted regulation of T cells by CD44. Commun Integr Biol 3: 508–512. [PubMed: 21331226]
107. Jung TM, Gallatin WM, Weissman IL, and Dailey MO. 1988 Down-regulation of homing receptors after T cell activation. J Immunol 141: 4110–4117. [PubMed: 3058798]
108. Linsley PS, Greene JL, Tan P, Bradshaw J, Ledbetter JA, Anasetti C, and Damle NK. 1992 Coexpression and functional cooperation of CTLA-4 and CD28 on activated T lymphocytes. J Exp Med 176: 1595–1604. [PubMed: 1334116]
109. Ahn E, Araki K, Hashimoto M, Li W, Riley JL, Cheung J, Sharpe AH, Freeman GJ, Irving BA, and Ahmed R. 2018 Role of PD-1 during effector CD8 T cell differentiation. Proc Natl Acad Sci U S A 115: 4749–4754. [PubMed: 29654146]
110. Samstag Y, Emmrich F, and Staehelin T. 1988 Activation of human T lymphocytes: differential effects of CD3- and CD8-mediated signals. Proc Natl Acad Sci U S A 85: 9689–9693. [PubMed: 2974160]
111. Kambayashi T, Assarsson E, Lukacher AE, Ljunggren HG, and Jensen PE. 2003 Memory CD8+ T cells provide an early source of IFN-gamma. J Immunol 170: 2399–2408. [PubMed: 12594263]
112. Harris DP, Goodrich S, Gerth AJ, Peng SL, and Lund FE. 2005 Regulation of IFN-gamma production by B effector 1 cells: essential roles for T-bet and the IFN-gamma receptor. J Immunol 174: 6781–6790. [PubMed: 15905519]
113. Chan T, Pek EA, Huth K, and Ashkar AA. 2011 CD4(+) T-cells are important in regulating macrophage polarization in C57BL/6 wild-type mice. Cell Immunol 266: 180–186. [PubMed: 21040907]
114. Heusinkveld M, de Vos van Steenwijk PJ, Goedemans R, Ramwadhdoebe TH, Gorter A, Welters MJ, van Hall T, and van der Burg SH. 2011 M2 macrophages induced by prostaglandin E2 and IL-6 from cervical carcinoma are switched to activated M1 macrophages by CD4+ Th1 cells. J Immunol 187: 1157–1165. [PubMed: 21709158]
115. Murray PJ, Allen JE, Biswas SK, Fisher EA, Gilroy DW, Goerdt S, Gordon S, Hamilton JA, Ivashkiv LB, Lawrence T, Locati M, Mantovani A, Martinez FO, Mege JL, Mosser DM, Natoli G, Saeij JP, Schultze JL, Shirey KA, Sica A, Suttles J, Udalova I, van Ginderachter JA, Vogel SN, and Wynn TA. 2014 Macrophage activation and polarization: nomenclature and experimental guidelines. Immunity 41: 14–20. [PubMed: 25035950]
116. Romero R, Quintero R, Nores J, Avila C, Mazor M, Hanaoka S, Hagay Z, Merchant L, and Hobbins JC. 1991 Amniotic fluid white blood cell count: a rapid and simple test to diagnose microbial invasion of the amniotic cavity and predict preterm delivery. Am J Obstet Gynecol 165: 821–830. [PubMed: 1951538]
117. Boldenow E, Gendrin C, Ngo L, Bierle C, Vornhagen J, Coleman M, Merillat S, Armistead B, Whidbey C, Alishetti V, Santana-Ufret V, Ogle J, Gough M, Srinouanprachanh S, MacDonald JW, Bammler TK, Bansal A, Liggitt HD, Rajagopal L, and Adams Waldorf KM. 2016 Group B Streptococcus circumvents neutrophils and neutrophil extracellular traps during amniotic cavity invasion and preterm labor. Sci Immunol 1.
118. Gomez-Lopez N, Romero R, Xu Y, Miller D, Unkel R, Shaman M, Jacques SM, Panaitescu B, Garcia-Flores V, and Hassan SS. 2017 Neutrophil Extracellular Traps in the Amniotic Cavity of Women with Intra-Amniotic Infection: A New Mechanism of Host Defense. Reprod Sci 24: 1139–1153. [PubMed: 27884950]

119. Gomez-Lopez N, Romero R, Leng Y, Garcia-Flores V, Xu Y, Miller D, and Hassan SS. 2017 Neutrophil extracellular traps in acute chorioamnionitis: A mechanism of host defense. Am J Reprod Immunol 77.
120. Gomez-Lopez N, Romero R, Garcia-Flores V, Xu Y, Leng Y, Alhousseini A, Hassan SS, and Panaitescu B. 2017 Amniotic fluid neutrophils can phagocytize bacteria: A mechanism for microbial killing in the amniotic cavity. Am J Reprod Immunol 78.
121. Gomez-Lopez N, Romero R, Xu Y, Leng Y, Garcia-Flores V, Miller D, Jacques SM, Hassan SS, Faro J, Alsamsam A, Alhousseini A, Gomez-Roberts H, Panaitescu B, Yeo L, and Maymon E. 2017 Are amniotic fluid neutrophils in women with intraamniotic infection and/or inflammation of fetal or maternal origin? Am J Obstet Gynecol 217: 693.e691–693.e616. [PubMed: 28964823]
122. Rinaldi SF, Catalano RD, Wade J, Rossi AG, and Norman JE. 2014 Decidual neutrophil infiltration is not required for preterm birth in a mouse model of infection-induced preterm labor. J Immunol 192: 2315–2325. [PubMed: 24501200]
123. Dudley DJ, Collmer D, Mitchell MD, and Trautman MS. 1996 Inflammatory cytokine mRNA in human gestational tissues: implications for term and preterm labor. J Soc Gynecol Investig 3: 328–335.
124. Shankar R, Johnson MP, Williamson NA, Cullinane F, Purcell AW, Moses EK, and Brennecke SP. 2010 Molecular markers of preterm labor in the choriodecidua. Reprod Sci 17: 297–310. [PubMed: 20009011]
125. Rinaldi SF, Makieva S, Saunders PT, Rossi AG, and Norman JE. 2017 Immune cell and transcriptomic analysis of the human decidua in term and preterm parturition. Mol Hum Reprod 23: 708–724. [PubMed: 28962035]
126. Bukowski R, Sadovsky Y, Goodarzi H, Zhang H, Biggio JR, Varner M, Parry S, Xiao F, Esplin SM, Andrews W, Saade GR, Ilekis JV, Reddy UM, and Baldwin DA. 2017 Onset of human preterm and term birth is related to unique inflammatory transcriptome profiles at the maternal fetal interface. PeerJ 5: e3685. [PubMed: 28879060]
127. Cook JL, Zaragoza DB, Sung DH, and Olson DM. 2000 Expression of myometrial activation and stimulation genes in a mouse model of preterm labor: myometrial activation, stimulation, and preterm labor. Endocrinology 141: 1718–1728. [PubMed: 10803582]
128. Tattersall M, Engineer N, Khanjani S, Sooranna SR, Roberts VH, Grigsby PL, Liang Z, Myatt L, and Johnson MR. 2008 Pro-labour myometrial gene expression: are preterm labour and term labour the same? Reproduction 135: 569–579. [PubMed: 18367515]
129. Migale R, MacIntyre DA, Cacciatore S, Lee YS, Hagberg H, Herbert BR, Johnson MR, Peebles D, Waddington SN, and Bennett PR. 2016 Modeling hormonal and inflammatory contributions to preterm and term labor using uterine temporal transcriptomics. BMC Med 14: 86. [PubMed: 27291689]
130. Makieva S, Dubicke A, Rinaldi SF, Fransson E, Ekman-Ordeberg G, and Norman JE. 2017 The preterm cervix reveals a transcriptomic signature in the presence of premature prelabor rupture of membranes. Am J Obstet Gynecol 216: 602 e601–602 e621. [PubMed: 28209491]
131. Gomez-Lopez N, Laresgoiti-Servitje E, Olson DM, Estrada-Gutierrez G, and Vadillo-Ortega F. 2010 The role of chemokines in term and premature rupture of the fetal membranes: a review. Biol Reprod 82: 809–814. [PubMed: 20089887]
132. Hamilton SA, Tower CL, and Jones RL. 2013 Identification of chemokines associated with the recruitment of decidual leukocytes in human labour: potential novel targets for preterm labour. PLoS One 8: e56946. [PubMed: 23451115]
133. Fischer DC, Winkler M, Ruck P, Poth D, Kemp B, and Rath W. 2001 Localization and quantification of adhesion molecule expression in the lower uterine segment during premature labor. J Perinat Med 29: 497–505. [PubMed: 11776680]
134. Winkler M, Kemp B, Fischer DC, Ruck P, and Rath W. 2003 Expression of adhesion molecules in the lower uterine segment during term and preterm parturition. Microsc Res Tech 60: 430–444. [PubMed: 12567400]
135. Gomez-Lopez N, Romero R, Xu Y, Plazyo O, Unkel R, Leng Y, Than NG, Chaiworapongsa T, Panaitescu B, Dong Z, Tarca AL, Abrahams VM, Yeo L, and Hassan SS. 2017 A Role for the

Inflammasome in Spontaneous Preterm Labor With Acute Histologic Chorioamnionitis. Reprod Sci 24: 1382–1401. [PubMed: 28122480]

136. Willcockson AR, Nandu T, Liu CL, Nallasamy S, Kraus WL, and Mahendroo M. 2018 Transcriptome signature identifies distinct cervical pathways induced in lipopolysaccharide-mediated preterm birth. Biol Reprod 98: 408–421. [PubMed: 29281003]
137. Timmons BC, Reese J, Socrate S, Ehinger N, Paria BC, Milne GL, Akins ML, Auchus RJ, McIntire D, House M, and Mahendroo M. 2014 Prostaglandins are essential for cervical ripening in LPS-mediated preterm birth but not term or antiprogestin-driven preterm ripening. Endocrinology 155: 287–298. [PubMed: 24189143]
138. Martinelli P, Sarno L, Maruotti GM, and Paludetto R. 2012 Chorioamnionitis and prematurity: a critical review. J Matern Fetal Neonatal Med 25 Suppl 4: 29–31. [PubMed: 22958008]
139. Oh KJ, Kim SM, Hong JS, Maymon E, Erez O, Panaitescu B, Gomez-Lopez N, Romero R, and Yoon BH. 2017 Twenty-four percent of patients with clinical chorioamnionitis in preterm gestations have no evidence of either culture-proven intraamniotic infection or intraamniotic inflammation. Am J Obstet Gynecol 216: 604 e601–604 e611. [PubMed: 28257964]
140. Gotsch F, Romero R, Espinoza J, Kusanovic JP, Mazaki-Tovi S, Erez O, Than NG, Edwin S, Mazor M, Yoon BH, and Hassan SS. 2007 Maternal serum concentrations of the chemokine CXCL10/IP-10 are elevated in acute pyelonephritis during pregnancy. J Matern Fetal Neonatal Med 20: 735–744. [PubMed: 17763275]
141. Madan I, Than NG, Romero R, Chaemsaithong P, Miranda J, Tarca AL, Bhatti G, Draghici S, Yeo L, Mazor M, Hassan SS, and Chaiworapongsa T. 2014 The peripheral whole-blood transcriptome of acute pyelonephritis in human pregnancya. J Perinat Med 42: 31–53. [PubMed: 24293448]
142. Olson DM, Zaragoza DB, Shallow MC, Cook JL, Mitchell BF, Grigsby P, and Hirst J. 2003 Myometrial activation and preterm labour: evidence supporting a role for the prostaglandin F receptor--a review. Placenta 24 Suppl A: S47–54. [PubMed: 12842413]
143. Romero R, Miranda J, Chaiworapongsa T, Korzeniewski SJ, Chaemsaithong P, Gotsch F, Dong Z, Ahmed AI, Yoon BH, Hassan SS, Kim CJ, and Yeo L. 2014 Prevalence and clinical significance of sterile intra-amniotic inflammation in patients with preterm labor and intact membranes. Am J Reprod Immunol 72: 458–474. [PubMed: 25078709]
144. Romero R, Miranda J, Chaemsaithong P, Chaiworapongsa T, Kusanovic JP, Dong Z, Ahmed AI, Shaman M, Lannaman K, Yoon BH, Hassan SS, Kim CJ, Korzeniewski SJ, Yeo L, and Kim YM. 2015 Sterile and microbial-associated intra-amniotic inflammation in preterm prelabor rupture of membranes. J Matern Fetal Neonatal Med 28: 1394–1409. [PubMed: 25190175]
145. Romero R, Grivel JC, Tarca AL, Chaemsaithong P, Xu Z, Fitzgerald W, Hassan SS, Chaiworapongsa T, and Margolis L. 2015 Evidence of perturbations of the cytokine network in preterm labor. Am J Obstet Gynecol 213: 836 e831–836 e818. [PubMed: 26232508]
146. Yoon BH, Romero R, Jun JK, Park KH, Park JD, Ghezzi F, and Kim BI. 1997 Amniotic fluid cytokines (interleukin-6, tumor necrosis factor-alpha, interleukin-1 beta, and interleukin-8) and the risk for the development of bronchopulmonary dysplasia. Am J Obstet Gynecol 177: 825–830. [PubMed: 9369827]
147. Ghezzi F, Gomez R, Romero R, Yoon BH, Edwin SS, David C, Janisse J, and Mazor M. 1998 Elevated interleukin-8 concentrations in amniotic fluid of mothers whose neonates subsequently develop bronchopulmonary dysplasia. Eur J Obstet Gynecol Reprod Biol 78: 5–10. [PubMed: 9605441]
148. Gomez R, Romero R, Ghezzi F, Yoon BH, Mazor M, and Berry SM. 1998 The fetal inflammatory response syndrome. Am J Obstet Gynecol 179: 194–202. [PubMed: 9704787]
149. Gussenhoven R, Westerlaken RJJ, Ophelders D, Jobe AH, Kemp MW, Kallapur SG, Zimmermann LJ, Sangild PT, Pankratova S, Gressens P, Kramer BW, Fleiss B, and Wolfs T. 2018 Chorioamnionitis, neuroinflammation, and injury: timing is key in the preterm ovine fetus. J Neuroinflammation 15: 113. [PubMed: 29673373]
150. Rueda CM, Presicce P, Jackson CM, Miller LA, Kallapur SG, Jobe AH, and Chougnet CA. 2016 Lipopolysaccharide-Induced Chorioamnionitis Promotes IL-1-Dependent Inflammatory FOXP3+ CD4+ T Cells in the Fetal Rhesus Macaque. J Immunol 196: 3706–3715. [PubMed: 27036917]

151. Matta P, Sherrod SD, Marasco CC, Moore DJ, McLean JA, and Weitkamp JH. 2017 In Utero Exposure to Histological Chorioamnionitis Primes the Exometabolomic Profiles of Preterm CD4(+) T Lymphocytes. J Immunol 199: 3074–3085. [PubMed: 28947540]

152. Inoue H, Nishio H, Takada H, Sakai Y, Nanishi E, Ochiai M, Onimaru M, Chen SJ, Matsui T, and Hara T. 2016 Activation of Nod1 Signaling Induces Fetal Growth Restriction and Death through Fetal and Maternal Vasculopathy. J Immunol 196: 2779–2787. [PubMed: 26880761]

153. Kallapur SG, Willet KE, Jobe AH, Ikegami M, and Bachurski CJ. 2001 Intra-amniotic endotoxin: chorioamnionitis precedes lung maturation in preterm lambs. Am J Physiol Lung Cell Mol Physiol 280: L527–536. [PubMed: 11159037]

154. Visconti K, Senthamaraikannan P, Kemp MW, Saito M, Kramer BW, Newnham JP, Jobe AH, and Kallapur SG. 2018 Extremely preterm fetal sheep lung responses to antenatal steroids and inflammation. Am J Obstet Gynecol 218: 349 e341–349 e310. [PubMed: 29274832]

155. Agrons GA, Courtney SE, Stocker JT, and Markowitz RI. 2005 From the archives of the AFIP: Lung disease in premature neonates: radiologic-pathologic correlation. Radiographics 25: 1047–1073. [PubMed: 16009823]

156. Warburton D, El-Hashash A, Carraro G, Tiozzo C, Sala F, Rogers O, De Langhe S, Kemp PJ, Riccardi D, Torday J, Bellusci S, Shi W, Lubkin SR, and Jesudason E. 2010 Lung organogenesis. Curr Top Dev Biol 90: 73–158. [PubMed: 20691848]

157. Mitchell BF, and Taggart MJ. 2009 Are animal models relevant to key aspects of human parturition? Am J Physiol Regul Integr Comp Physiol 297: R525–545. [PubMed: 19515978]

158. Nadeem L, Shynlova O, Matysiak-Zablocki E, Mesiano S, Dong X, and Lye S. 2016 Molecular evidence of functional progesterone withdrawal in human myometrium. Nat Commun 7: 11565. [PubMed: 27220952]

159. Meis PJ, Klebanoff M, Thom E, Dombrowski MP, Sibai B, Moawad AH, Spong CY, Hauth JC, Miodovnik M, Varner MW, Leveno KJ, Caritis SN, Iams JD, Wapner RJ, Conway D, O'Sullivan MJ, Carpenter M, Mercer B, Ramin SM, Thorp JM, Peaceman AM, Gabbe S, H. National Institute of Child, and N. Human Development Maternal-Fetal Medicine Units. 2003 Prevention of recurrent preterm delivery by 17 alpha-hydroxyprogesterone caproate. N Engl J Med 348: 2379–2385. [PubMed: 12802023]

160. da Fonseca EB, Bittar RE, Carvalho MH, and Zugaib M. 2003 Prophylactic administration of progesterone by vaginal suppository to reduce the incidence of spontaneous preterm birth in women at increased risk: a randomized placebo-controlled double-blind study. Am J Obstet Gynecol 188: 419–424. [PubMed: 12592250]

161. O'Brien JM, Adair CD, Lewis DF, Hall DR, Defranco EA, Fusey S, Soma-Pillay P, Porter K, How H, Schackis R, Eller D, Trivedi Y, Vanburen G, Khandelwal M, Trofatter K, Vidyadhari D, Vijayaraghavan J, Weeks J, Dattel B, Newton E, Chazotte C, Valenzuela G, Calda P, Bsharat M, and Creasy GW. 2007 Progesterone vaginal gel for the reduction of recurrent preterm birth: primary results from a randomized, double-blind, placebo-controlled trial. Ultrasound Obstet Gynecol 30: 687–696. [PubMed: 17899572]

162. Fonseca EB, Celik E, Parra M, Singh M, Nicolaides KH, and Fetal G Medicine Foundation Second Trimester Screening. 2007 Progesterone and the risk of preterm birth among women with a short cervix. N Engl J Med 357: 462–469. [PubMed: 17671254]

163. Hassan SS, Romero R, Vidyadhari D, Fusey S, Baxter JK, Khandelwal M, Vijayaraghavan J, Trivedi Y, Soma-Pillay P, Sambarey P, Dayal A, Potapov V, O'Brien J, Astakhov V, Yuzko O, Kinzler W, Dattel B, Sehdev H, Mazheika L, Manchulenko D, Gervasi MT, Sullivan L, Conde-Agudelo A, Phillips JA, Creasy GW, and Trial P. 2011 Vaginal progesterone reduces the rate of preterm birth in women with a sonographic short cervix: a multicenter, randomized, double-blind, placebo-controlled trial. Ultrasound Obstet Gynecol 38: 18–31. [PubMed: 21472815]

164. Yee LM, Liu LY, Sakowicz A, Bolden JR, and Miller ES. 2016 Racial and ethnic disparities in use of 17-alpha hydroxyprogesterone caproate for prevention of preterm birth. Am J Obstet Gynecol 214: 374 e371–376. [PubMed: 26829989]

165. Norman JE, Marlow N, Messow CM, Shennan A, Bennett PR, Thornton S, Robson SC, McConnachie A, Petrou S, Sebire NJ, Lavender T, Whyte S, Norrie J, and O. s. group. 2016 Vaginal progesterone prophylaxis for preterm birth (the OPPTIMUM study): a multicentre, randomised, double-blind trial. Lancet 387: 2106–2116. [PubMed: 26921136]

166. Society for Maternal-Fetal Medicine Publications, C. 2017 The choice of progestogen for the prevention of preterm birth in women with singleton pregnancy and prior preterm birth. Am J Obstet Gynecol 216: B11–B13. [PubMed: 28126367]

167. Romero R, Conde-Agudelo A, Da Fonseca E, O'Brien JM, Cetingoz E, Creasy GW, Hassan SS, and Nicolaides KH. 2018 Vaginal progesterone for preventing preterm birth and adverse perinatal outcomes in singleton gestations with a short cervix: a meta-analysis of individual patient data. Am J Obstet Gynecol 218: 161–180. [PubMed: 29157866]

168. Furcron AE, Romero R, Plazyo O, Unkel R, Xu Y, Hassan SS, Chaemsaithong P, Mahajan A, and Gomez-Lopez N. 2015 Vaginal progesterone, but not 17alpha-hydroxyprogesterone caproate, has antiinflammatory effects at the murine maternal-fetal interface. Am J Obstet Gynecol 213: 846 e841–846 e819. [PubMed: 26264823]

169. Elovitz MA, and Mrinalini C. 2006 The use of progestational agents for preterm birth: lessons from a mouse model. Am J Obstet Gynecol 195: 1004–1010. [PubMed: 17000233]

170. Elovitz MA, and Gonzalez J. 2008 Medroxyprogesterone acetate modulates the immune response in the uterus, cervix and placenta in a mouse model of preterm birth. J Matern Fetal Neonatal Med 21: 223–230. [PubMed: 18330817]

171. Gomez-Lopez N, Hernandez-Santiago S, Lobb AP, Olson DM, and Vadillo-Ortega F. 2013 Normal and premature rupture of fetal membranes at term delivery differ in regional chemotactic activity and related chemokine/cytokine production. Reprod Sci 20: 276–284. [PubMed: 22836164]

172. Sindram-Trujillo A, Scherjon S, Kanhai H, Roelen D, and Claas F. 2003 Increased T-cell activation in decidua parietalis compared to decidua basalis in uncomplicated human term pregnancy. Am J Reprod Immunol 49: 261–268. [PubMed: 12854730]

173. Sindram-Trujillo AP, Scherjon SA, van Hulst-van Miert PP, Kanhai HH, Roelen DL, and Claas FH. 2004 Comparison of decidual leukocytes following spontaneous vaginal delivery and elective cesarean section in uncomplicated human term pregnancy. J Reprod Immunol 62: 125–137. [PubMed: 15288188]

174. Tilburgs T, Roelen DL, van der Mast BJ, van Schip JJ, Kleijburg C, de Groot-Swings GM, Kanhai HH, Claas FH, and Scherjon SA. 2006 Differential distribution of CD4(+)CD25(bright) and CD8(+)CD28(−) T-cells in decidua and maternal blood during human pregnancy. Placenta 27 Suppl A: S47–53. [PubMed: 16442616]

175. Tilburgs T, Scherjon SA, Roelen DL, and Claas FH. 2009 Decidual CD8+CD28− T cells express CD103 but not perforin. Hum Immunol 70: 96–100. [PubMed: 19150377]

176. Tilburgs T, van der Mast BJ, Nagtzaam NM, Roelen DL, Scherjon SA, and Claas FH. 2009 Expression of NK cell receptors on decidual T cells in human pregnancy. J Reprod Immunol 80: 22–32. [PubMed: 19394706]

177. Tilburgs T, Schonkeren D, Eikmans M, Nagtzaam NM, Datema G, Swings GM, Prins F, van Lith JM, van der Mast BJ, Roelen DL, Scherjon SA, and Claas FH. 2010 Human decidual tissue contains differentiated CD8+ effector-memory T cells with unique properties. J Immunol 185: 4470–4477. [PubMed: 20817873]

178. Powell RM, Lissauer D, Tamblyn J, Beggs A, Cox P, Moss P, and Kilby MD. 2017 Decidual T Cells Exhibit a Highly Differentiated Phenotype and Demonstrate Potential Fetal Specificity and a Strong Transcriptional Response to IFN. J Immunol 199: 3406–3417. [PubMed: 28986438]

179. van der Zwan A, Bi K, Norwitz ER, Crespo AC, Claas FHJ, Strominger JL, and Tilburgs T. 2018 Mixed signature of activation and dysfunction allows human decidual CD8(+) T cells to provide both tolerance and immunity. Proc Natl Acad Sci U S A 115: 385–390. [PubMed: 29259116]

180. Unutmaz D, Pileri P, and Abrignani S. 1994 Antigen-independent activation of naive and memory resting T cells by a cytokine combination. J Exp Med 180: 1159–1164. [PubMed: 8064232]

181. Norton MT, Fortner KA, Oppenheimer KH, and Bonney EA. 2010 Evidence that CD8 T-cell homeostasis and function remain intact during murine pregnancy. Immunology 131: 426–437. [PubMed: 20553337]

182. Hamann D, Baars PA, Rep MH, Hooibrink B, Kerkhof-Garde SR, Klein MR, and van Lier RA. 1997 Phenotypic and functional separation of memory and effector human CD8+ T cells. J Exp Med 186: 1407–1418. [PubMed: 9348298]

183. Shresta S, Pham CT, Thomas DA, Graubert TA, and Ley TJ. 1998 How do cytotoxic lymphocytes kill their targets? Curr Opin Immunol 10: 581–587. [PubMed: 9794837]

184. Trapani JA, and Smyth MJ. 2002 Functional significance of the perforin/granzyme cell death pathway. Nat Rev Immunol 2: 735–747. [PubMed: 12360212]

185. Trambas CM, and Griffiths GM. 2003 Delivering the kiss of death. Nat Immunol 4: 399–403. [PubMed: 12719728]

186. Takata H, and Takiguchi M. 2006 Three memory subsets of human CD8+ T cells differently expressing three cytolytic effector molecules. J Immunol 177: 4330–4340. [PubMed: 16982867]

187. Ferran C, Dy M, Sheehan K, Merite S, Schreiber R, Landais P, Grau G, Bluestone J, Bach JF, and Chatenoud L. 1991 Inter-mouse strain differences in the in vivo anti-CD3 induced cytokine release. Clin Exp Immunol 86: 537–543. [PubMed: 1721015]

188. Minami Y, Samelson LE, and Klausner RD. 1987 Internalization and cycling of the T cell antigen receptor. Role of protein kinase C. J Biol Chem 262: 13342–13347. [PubMed: 3498715]

189. von Essen M, Bonefeld CM, Siersma V, Rasmussen AB, Lauritsen JP, Nielsen BL, and Geisler C. 2004 Constitutive and ligand-induced TCR degradation. J Immunol 173: 384–393. [PubMed: 15210797]

190. Lal G, Shaila MS, and Nayak R. 2006 Activated mouse T cells downregulate, process and present their surface TCR to cognate anti-idiotypic CD4+ T cells. Immunol Cell Biol 84: 145–153. [PubMed: 16519732]

191. Tamura T, and Nariuchi H. 1992 T cell activation through TCR/-CD3 complex. IL-2 production of T cell clones stimulated with anti-CD3 without cross-linkage. J Immunol 148: 2370–2377. [PubMed: 1532813]

192. Ashkar AA, Di Santo JP, and Croy BA. 2000 Interferon gamma contributes to initiation of uterine vascular modification, decidual integrity, and uterine natural killer cell maturation during normal murine pregnancy. J Exp Med 192: 259–270. [PubMed: 10899912]

193. Frascoli M, Coniglio L, Witt R, Jeanty C, Fleck-Derderian S, Myers DE, Lee TH, Keating S, Busch MP, Norris PJ, Tang Q, Cruz G, Barcellos LF, Gomez-Lopez N, Romero R, and MacKenzie TC. 2018 Alloreactive fetal T cells promote uterine contractility in preterm labor via IFN-gamma and TNF-alpha. Sci Transl Med 10.

194. Xue J, Schmidt SV, Sander J, Draffehn A, Krebs W, Quester I, De Nardo D, Gohel TD, Emde M, Schmidleithner L, Ganesan H, Nino-Castro A, Mallmann MR, Labzin L, Theis H, Kraut M, Beyer M, Latz E, Freeman TC, Ulas T, and Schultze JL. 2014 Transcriptome-based network analysis reveals a spectrum model of human macrophage activation. Immunity 40: 274–288. [PubMed: 24530056]

195. Houser BL, Tilburgs T, Hill J, Nicotra ML, and Strominger JL. 2011 Two unique human decidual macrophage populations. J Immunol 186: 2633–2642. [PubMed: 21257965]

196. Natoli G, and Monticelli S. 2014 Macrophage activation: glancing into diversity. Immunity 40: 175–177. [PubMed: 24560195]

197. Mosser DM, and Edwards JP. 2008 Exploring the full spectrum of macrophage activation. Nat Rev Immunol 8: 958–969. [PubMed: 19029990]

198. Shynlova O, Nedd-Roderique T, Li Y, Dorogin A, and Lye SJ. 2013 Myometrial immune cells contribute to term parturition, preterm labour and post-partum involution in mice. J Cell Mol Med 17: 90–102. [PubMed: 23205502]

199. Shynlova O, Nedd-Roderique T, Li Y, Dorogin A, Nguyen T, and Lye SJ. 2013 Infiltration of myeloid cells into decidua is a critical early event in the labour cascade and post-partum uterine remodelling. J Cell Mol Med 17: 311–324. [PubMed: 23379349]

200. Presicce P, Park CW, Senthamaraikannan P, Bhattacharyya S, Jackson C, Kong F, Rueda CM, DeFranco E, Miller LA, Hildeman DA, Salomonis N, Chougnet CA, Jobe AH, and Kallapur SG. 2018 IL-1 signaling mediates intrauterine inflammation and chorio-decidua neutrophil recruitment and activation. JCI Insight 3.

201. Gomez R, Romero R, Edwin SS, and David C. 1997 Pathogenesis of preterm labor and preterm premature rupture of membranes associated with intraamniotic infection. Infect Dis Clin North Am 11: 135–176. [PubMed: 9067790]

202. Romero R, Gotsch F, Pineles B, and Kusanovic JP. 2007 Inflammation in pregnancy: its roles in reproductive physiology, obstetrical complications, and fetal injury. Nutr Rev 65: S194–202. [PubMed: 18240548]

203. El-Shazly S, Makhseed M, Azizieh F, and Raghupathy R. 2004 Increased expression of pro-inflammatory cytokines in placentas of women undergoing spontaneous preterm delivery or premature rupture of membranes. Am J Reprod Immunol 52: 45–52. [PubMed: 15214942]

204. Park CW, Yoon BH, Park JS, and Jun JK. 2013 An elevated maternal serum C-reactive protein in the context of intra-amniotic inflammation is an indicator that the development of amnionitis, an intense fetal and AF inflammatory response are likely in patients with preterm labor: clinical implications. J Matern Fetal Neonatal Med 26: 847–853. [PubMed: 23484918]

205. Cobo T, Tsiartas P, Kacerovsky M, Holst RM, Hougaard DM, Skogstrand K, Wennerholm UB, Hagberg H, and Jacobsson B. 2013 Maternal inflammatory response to microbial invasion of the amniotic cavity: analyses of multiple proteins in the maternal serum. Acta Obstet Gynecol Scand 92: 61–68. [PubMed: 23057959]

206. Tency I 2014 Inflammatory response in maternal serum during preterm labour. Facts Views Vis Obgyn 6: 19–30. [PubMed: 25009722]

207. Miech RP 2007 Pathopharmacology of excessive hemorrhage in mifepristone abortions. Ann Pharmacother 41: 2002–2007. [PubMed: 17956963]

208. Blois SM, Joachim R, Kandil J, Margni R, Tometten M, Klapp BF, and Arck PC. 2004 Depletion of CD8+ cells abolishes the pregnancy protective effect of progesterone substitution with dydrogesterone in mice by altering the Th1/Th2 cytokine profile. J Immunol 172: 5893–5899. [PubMed: 15128769]

209. Solano ME, Kowal MK, O'Rourke GE, Horst AK, Modest K, Plosch T, Barikbin R, Remus CC, Berger RG, Jago C, Ho H, Sass G, Parker VJ, Lydon JP, DeMayo FJ, Hecher K, Karimi K, and Arck PC. 2015 Progesterone and HMOX-1 promote fetal growth by CD8+ T cell modulation. J Clin Invest 125: 1726–1738. [PubMed: 25774501]

210. Swaims-Kohlmeier A, Haaland RE, Haddad LB, Sheth AN, Evans-Strickfaden T, Lupo LD, Cordes S, Aguirre AJ, Lupoli KA, Chen CY, Ofotukun I, Hart CE, and Kohlmeier JE. 2016 Progesterone Levels Associate with a Novel Population of CCR5+CD38+ CD4 T Cells Resident in the Genital Mucosa with Lymphoid Trafficking Potential. J Immunol 197: 368–376. [PubMed: 27233960]

211. Cross SN, Potter JA, Aldo P, Kwon JY, Pitruzzello M, Tong M, Guller S, Rothlin CV, Mor G, and Abrahams VM. 2017 Viral Infection Sensitizes Human Fetal Membranes to Bacterial Lipopolysaccharide by MERTK Inhibition and Inflammasome Activation. J Immunol 199: 2885–2895. [PubMed: 28916522]

212. Faro J, Romero R, Schwenkel G, Garcia-Flores V, Arenas-Hernandez M, Leng Y, Xu Y, Miller D, Hassan SS, and Gomez-Lopez N. 2018 Inflammation-Induced Intra-Amniotic inflammation induces preterm birth by Activating the NLRP3 inflammasome. Biol Reprod.

213. Gomez-Lopez N, Romero R, Garcia-Flores V, Leng Y, Miller D, Hassan SS, Hsu CD, and Panaitescu B. 2018 Inhibition of the NLRP3 inflammasome can prevent sterile intra-amniotic inflammation, preterm labor/birth and adverse neonatal outcomes. Biol Reprod.

214. Gomez-Lopez N, Romero R, Panaitescu B, Leng Y, Xu Y, Tarca AL, Faro J, Pacora P, Hassan SS, and Hsu CD. 2018 Inflammasome activation during spontaneous preterm labor with intra-amniotic infection or sterile intra-amniotic inflammation. Am J Reprod Immunol 80: e13049. [PubMed: 30225853]

215. Erlebacher A, Vencato D, Price KA, Zhang D, and Glimcher LH. 2007 Constraints in antigen presentation severely restrict T cell recognition of the allogeneic fetus. J Clin Invest 117: 1399–1411. [PubMed: 17446933]

216. Stout MJ, Conlon B, Landeau M, Lee I, Bower C, Zhao Q, Roehl KA, Nelson DM, Macones GA, and Mysorekar IU. 2013 Identification of intracellular bacteria in the basal plate of the human placenta in term and preterm gestations. Am J Obstet Gynecol 208: 226 e221–227. [PubMed: 23333552]

217. Moreno I, Codoner FM, Vilella F, Valbuena D, Martinez-Blanch JF, Jimenez-Almazan J, Alonso R, Alama P, Remohi J, Pellicer A, Ramon D, and Simon C. 2016 Evidence that the endometrial

microbiota has an effect on implantation success or failure. Am J Obstet Gynecol 215: 684–703. [PubMed: 27717732]

218. Kim CJ, Romero R, Chaemsaithong P, Chaiyasit N, Yoon BH, and Kim YM. 2015 Acute chorioamnionitis and funisitis: definition, pathologic features, and clinical significance. Am J Obstet Gynecol 213: S29–52. [PubMed: 26428501]
219. Gomez-Lopez N, Romero R, Panaitescu B, Leng Y, Xu Y, Tarca AL, Faro J, Pacora P, Hassan SS, and Hsu CD. 2018 Inflammasome activation during spontaneous preterm labor with intra-amniotic infection or sterile intra-amniotic inflammation. Am J Reprod Immunol: e13049. [PubMed: 30225853]
220. Cardenas I, Mor G, Aldo P, Lang SM, Stabach P, Sharp A, Romero R, Mazaki-Tovi S, Gervasi M, and Means RE. 2011 Placental viral infection sensitizes to endotoxin-induced pre-term labor: a double hit hypothesis. Am J Reprod Immunol 65: 110–117. [PubMed: 20712808]
221. Racicot K, Cardenas I, Wunsche V, Aldo P, Guller S, Means RE, Romero R, and Mor G. 2013 Viral infection of the pregnant cervix predisposes to ascending bacterial infection. J Immunol 191: 934–941. [PubMed: 23752614]
222. Racicot K, Kwon JY, Aldo P, Abrahams V, El-Guindy A, Romero R, and Mor G. 2016 Type I Interferon Regulates the Placental Inflammatory Response to Bacteria and is Targeted by Virus: Mechanism of Polymicrobial Infection-Induced Preterm Birth. Am J Reprod Immunol 75: 451–460. [PubMed: 26892235]

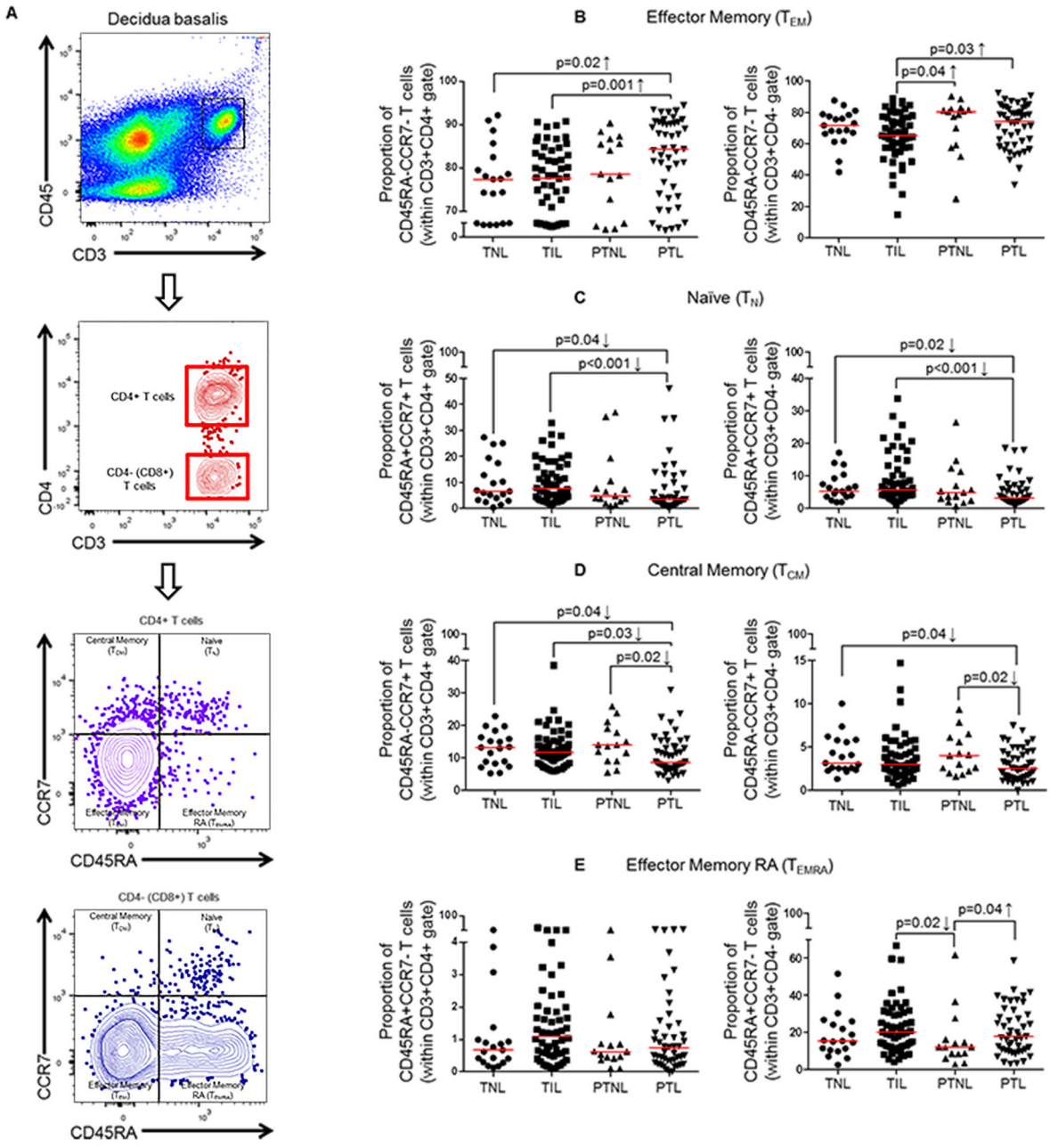

Fig. 1. Immunophenotyping of effector memory T cells in decidual tissues.

(**A**) Gating strategy used to identify CD4+ and CD4− (CD8+) effector memory (T_{EM}; CD45RA−CCR7−), naïve (T_N; CD45RA+CCR7+), central memory (T_{CM}; CD45RA −CCR7+) and effector memory RA (T_{EMRA}; CD45RA+ CCR7−) T cells in the decidua basalis from women who delivered at term without labor (TNL), term with labor (TIL), preterm without labor (PTNL), or preterm with labor (PTL). (**B**) Proportions of T_{EM} cells. (**C**) Proportions of T_N cells. (**D**) Proportions of T_{CM} cells. (**E**) Proportions of T_{EMRA} cells. The p-values were determined by 2-tailed Mann-Whitney *U*-test. Data are shown as scatter plots (median). Demographic and clinical characteristics of the study population are shown in Table I.

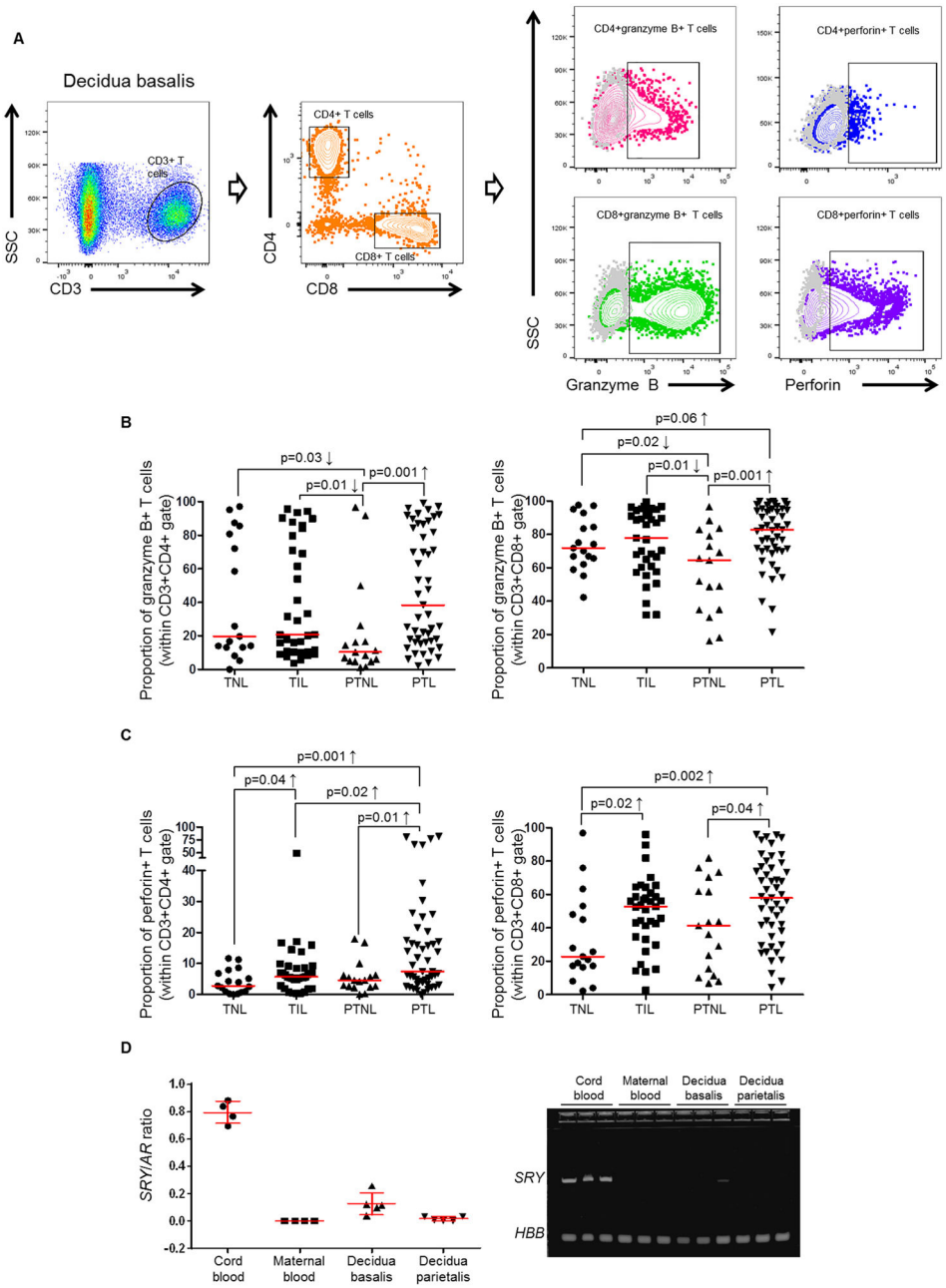

Fig. 2. Immunophenotyping of activated T cells in decidual tissues.

(**A**) Gating strategy used to identify CD4+ and CD8+ T cells expressing granzyme B or perforin in the decidua basalis from women who delivered at term without labor (TNL), term with labor (TIL), preterm without labor (PTNL), or preterm with labor (PTL). (**B**) Proportions of CD4+granzyme B+ or CD8+granzyme B+ T cells. (**C**) Proportions of CD4+perforin+ or CD8+perforin+ T cells. The p-values were determined by 2-tailed Mann-Whitney *U*-test. Data are shown as scatter plots (median). Demographic and clinical characteristics of the study population are shown in Table II. (**D**) qPCR ratio of *SRY* (Y-chromosome) to *AR* (X-chromosome) expression in CD3+ T cells isolated from umbilical cord blood, maternal peripheral blood, the decidua basalis, and the decidua parietalis. Data

are shown as scatter plots (median + interquartile range). Gel image of amplified PCR fragments shows *SRY* expression by CD3+ T cells isolated from umbilical cord blood, maternal peripheral blood, the decidua basalis, and the decidua parietalis. *HBB* = human β-globin (housekeeping gene).

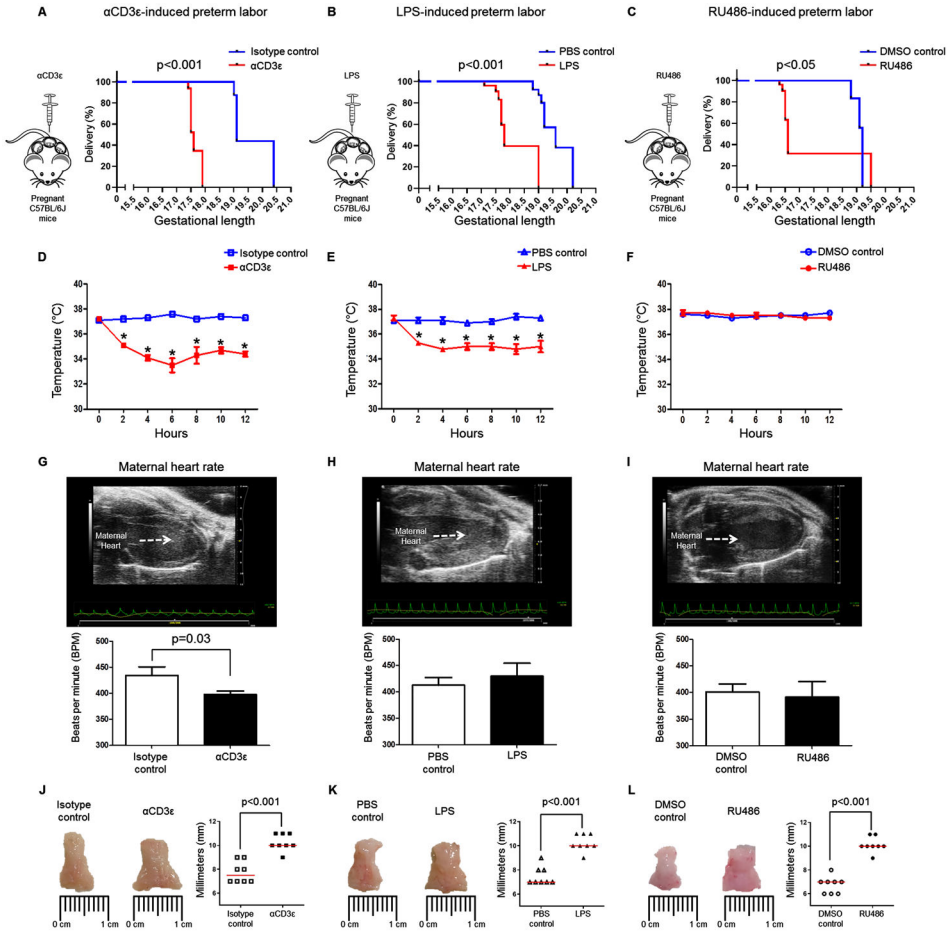

Fig. 3. Clinical parameters prior to preterm birth.

Kaplan-Meier survival curves showing the gestational length of dams injected with (**A**) αCD3ε (or isotype control), (**B**) LPS (or PBS control), or (**C**) RU486 (or DMSO control); n=3-8 each. The p-values were determined by Mantel-Cox test. The body temperature of the dams was recorded prior to and after the injection of (**D**) αCD3ε (■) or isotype control (□); (**E**) LPS (▲) or PBS control (Δ); (**F**) RU486 (●) or DMSO control (○). The p-values were determined by 2-tailed Mann-Whitney *U*-test. Data are shown as mean ± SEM; n=5 each, *p<0.01. Doppler ultrasound was performed on dams just prior to (**G**) αCD3ε-induced, (**H**) LPS-induced, or (**I**) RU486-induced preterm labor/birth. Maternal heart rate was evaluated by the mean of three constant waves of the uterine artery. The p-values were determined by 2-tailed unpaired *t*-test. Data are shown as mean ± SEM; n=6-17 each. Representative images and widths of the cervices collected from dams after injection with (**J**) αCD3ε or isotype control; (**K**) LPS or PBS control; or (**L**) RU486 or DMSO control. The p-values were determined by 2-tailed Mann-Whitney *U*-test. Data are shown as medians; n=8 each.

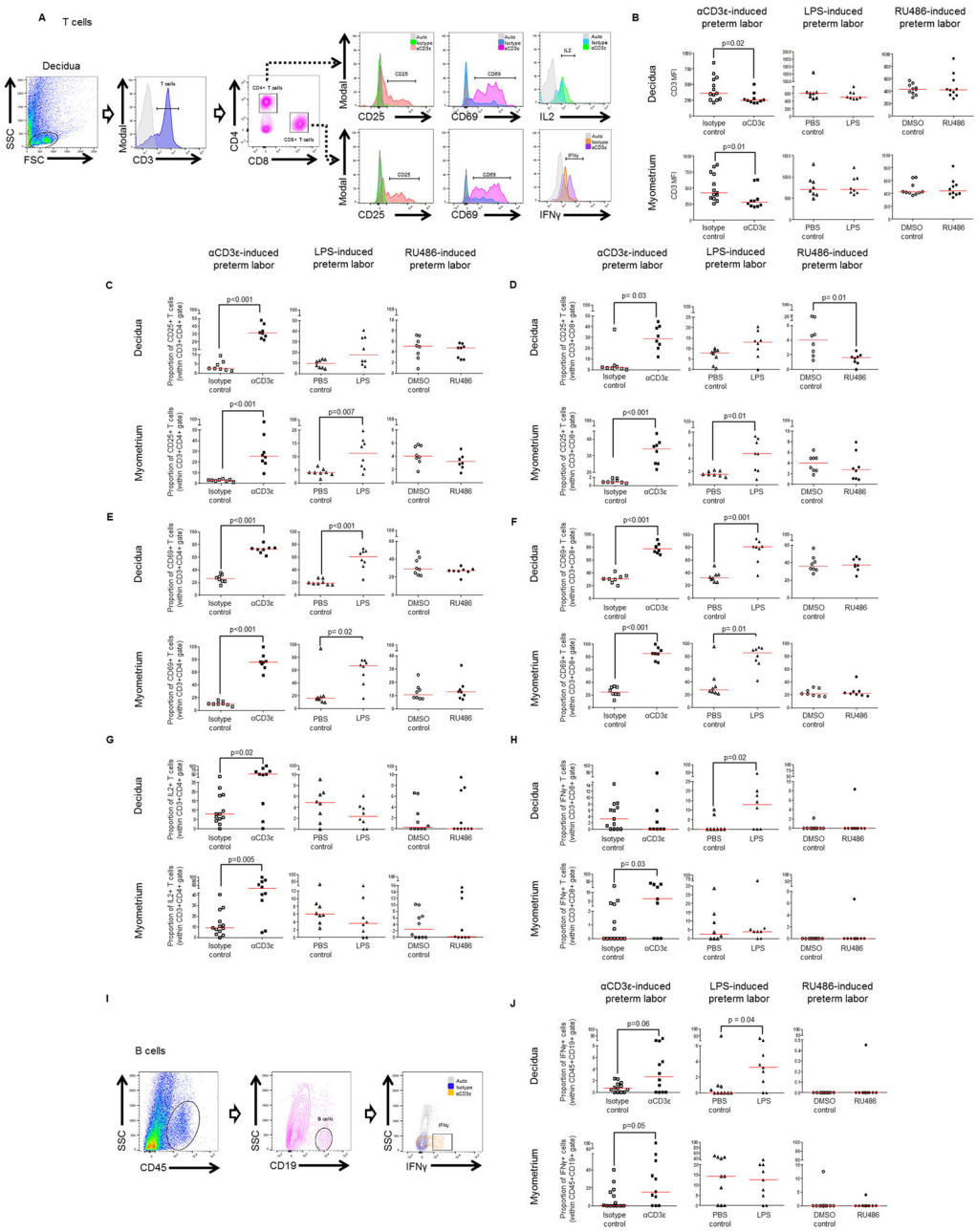

Fig. 4. Activation of T and B cells at the maternal-fetal interface and myometrium prior to preterm birth.

(**A**) Gating strategy used to identify activated CD4+ (CD3+CD4+ cells expressing CD25, CD69, or IL2) and CD8+ (CD3+CD8+ cells expressing CD25, CD69, or IFNγ) T cells at the maternal-fetal interface. Grey histograms represent autofluorescence controls, and colored histograms represent the expression of the CD3 molecule as well as CD25, CD69, IL2, or IFNγ. (**B**) Mean fluorescence intensity (MFI) of the CD3 molecule in decidual and myometrial tissues from dams injected with αCD3ε, isotype, LPS, PBS, RU486 or DMSO (n=8-13 each). Proportions of (**C**) CD4+ and (**D**) CD8+ T cells expressing CD25 in decidual and myometrial tissues from dams injected with αCD3ε, isotype, LPS, PBS, RU486, or

DMSO (n=8 each). Proportions of (**E**) CD4+ and (**F**) CD8+ T cells expressing CD69 in decidual and myometrial tissues from dams injected with αCD3ε, isotype, LPS, PBS, RU486, or DMSO (n=8 each). (**G**) Proportion of CD4+ T cells expressing IL2 in decidual and myometrial tissues from dams injected with αCD3ε, isotype, LPS, PBS, RU486, or DMSO (n=8-13 each). (**H**) Proportion of CD8+ T cells expressing IFNγ in decidual and myometrial tissues from dams injected with αCD3ε, isotype, LPS, PBS, RU486 or DMSO (n=8-13). (**I**) Gating strategy used to identify activated B cells (CD45+CD19+IFNγ+) at the maternal-fetal interface. The grey contour plot represents the autofluorescence control and the colored contour plot represents the expression of IFNγ. (**J**) Proportion of B cells expressing IFNγ in decidual or myometrial tissues from dams injected with αCD3ε, isotype, LPS, PBS, RU486 or DMSO (n=9-13 each). The p-values were determined by 2-tailed Mann-Whitney *U*-test. Data are shown as scatter plots (median).

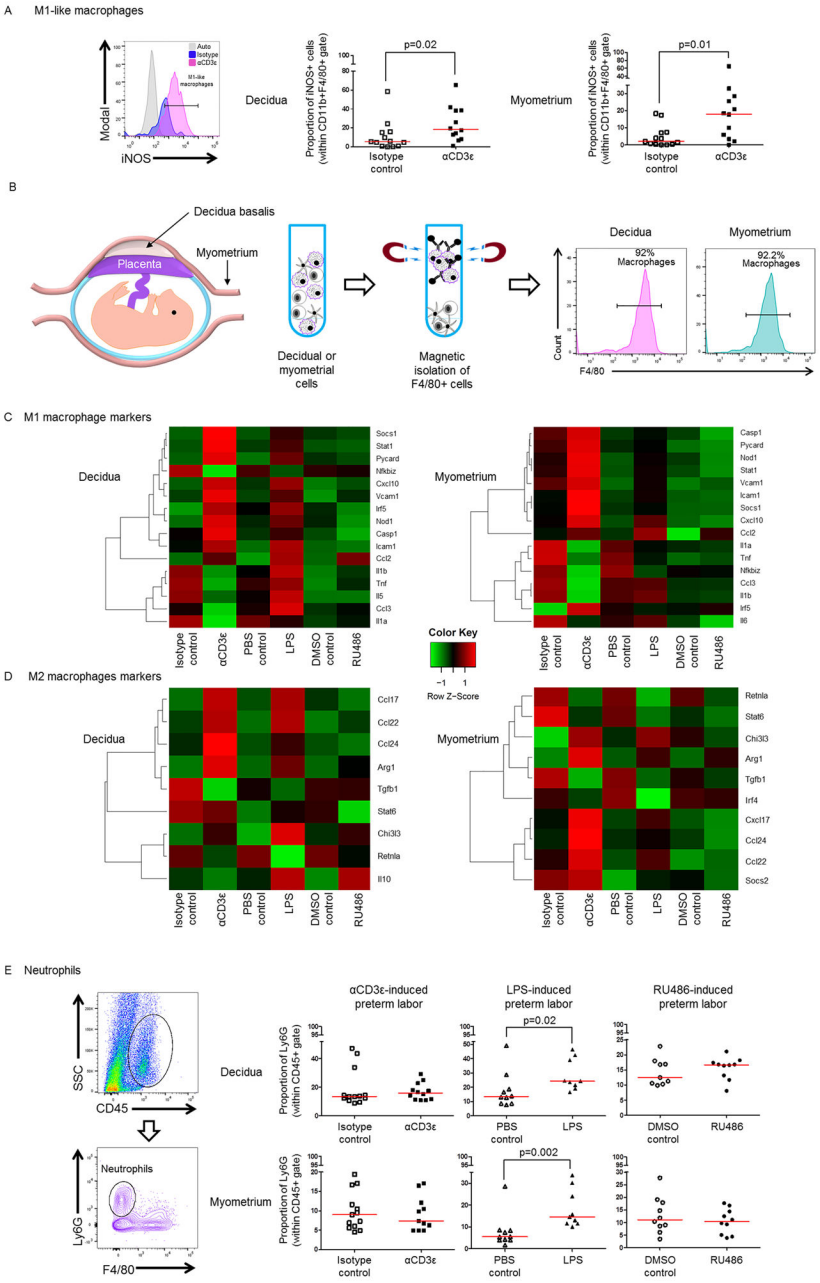

Fig. 5. A pro-inflammatory macrophage polarization but not a neutrophilic influx at the maternal-fetal interface and myometrium prior to *in vivo* T-cell activation-induced preterm birth.

(**A**) Gating strategy used to identify M1-like (CD11b+F4/80+iNOS+ cells) macrophages at the maternal-fetal interface. Grey histograms represent autofluorescence controls and colored histograms represent the expression of iNOS at the maternal-fetal interface of dams injected with isotype control or αCD3ε, respectively. Proportions of M1-like macrophages in the decidual and myometrial tissues from dams injected with αCD3ε or isotype, (n=12-13 each). (**B**) Left to right: spatial localization of the murine decidua and myometrium. Workflow showing the magnetic isolation of macrophages from decidual and myometrial

cells; macrophage purity (F4/80+ cells; >92%) was determined by flow cytometry. (**C**) Heat map visualization of the expression of M1 macrophage markers by F4/80+ cells isolated from the decidual and myometrial tissues of dams injected with αCD3ε, isotype, LPS, PBS, RU486 or DMSO (n=6-8 each). (**D**) Heat map visualization of the expression of M2 macrophage markers by F4/80+ cells isolated from the decidual and myometrial tissues of dams injected with αCD3ε, isotype, LPS, PBS, RU486 or DMSO (n=6-8 each). Negative (−)ΔCt values were calculated using *Actb*, *Gusb*, *Gapdh* and *Hsp90ab1* as reference genes. (**E**) Gating strategy used to identify neutrophils (CD45+Ly6G+ cells) at the maternal-fetal interface. Proportion of neutrophils in decidual and myometrial tissues from dams injected with αCD3ε, isotype, LPS, PBS, RU486 or DMSO (n=9-13 each). The p-values were determined by 2-tailed Mann-Whitney *U*-test. Data are shown as scatter plots (median).

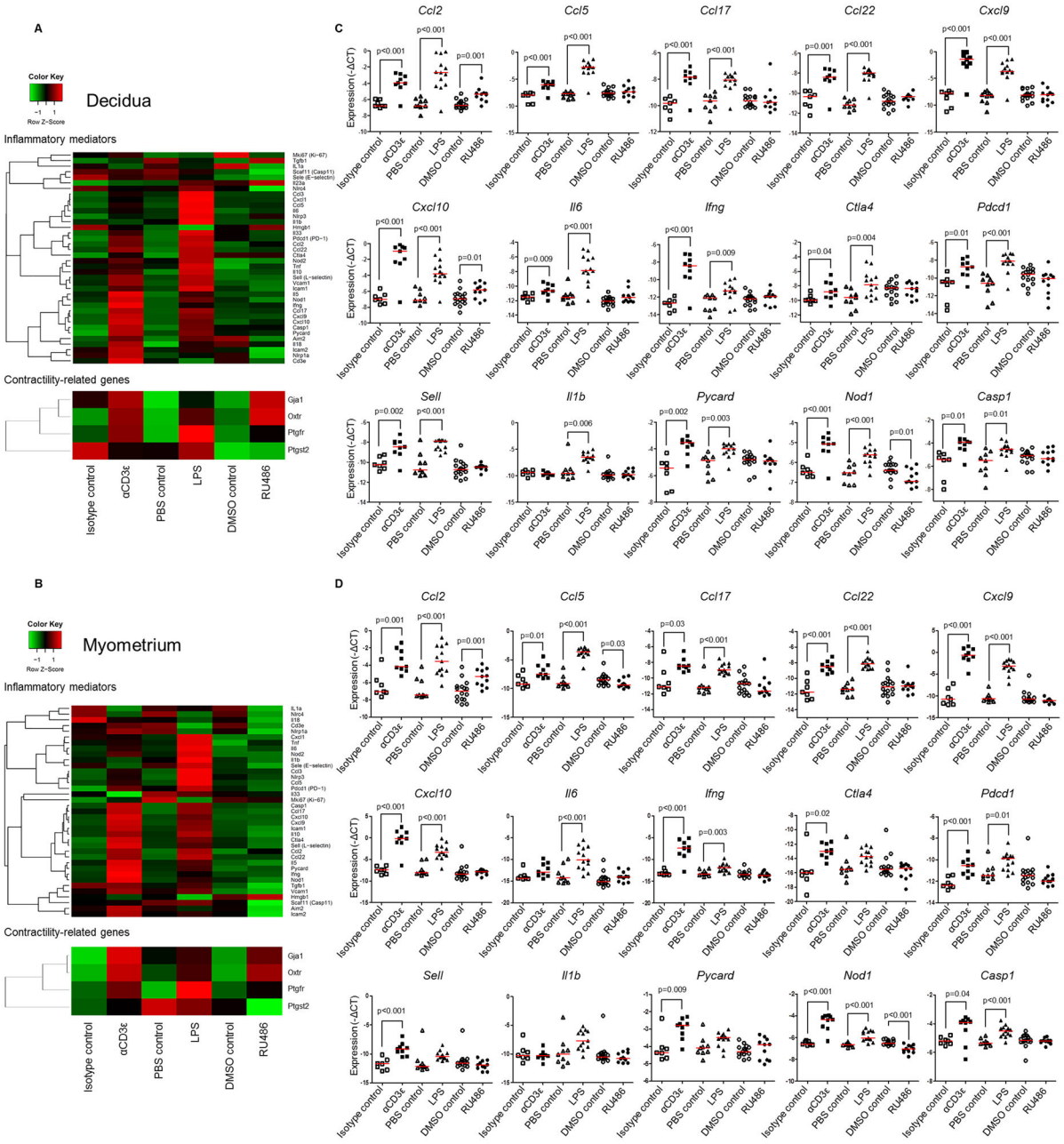

Fig. 6. Inflammatory gene expression at the maternal-fetal interface and myometrium prior to preterm birth.

Decidual and myometrial tissues from dams injected with αCD3ε (or isotype control), LPS (or PBS control), or RU486 (or DMSO control). Heat map visualization of inflammatory and contractility-related gene expression in the (**A**) decidual and (**B**) myometrial tissues. (**C&D**) Messenger (m)RNA expression of selected genes in decidual and myometrial tissues. Negative (−)ΔCt values were calculated using *Actb, Gusb, Gapdh* and *Hsp90ab1* as reference genes. Data are from individual dams (n=7-16 each). The p-values were determined by unpaired 2-tailed *t*-test. Data are shown as scatter plots (median).

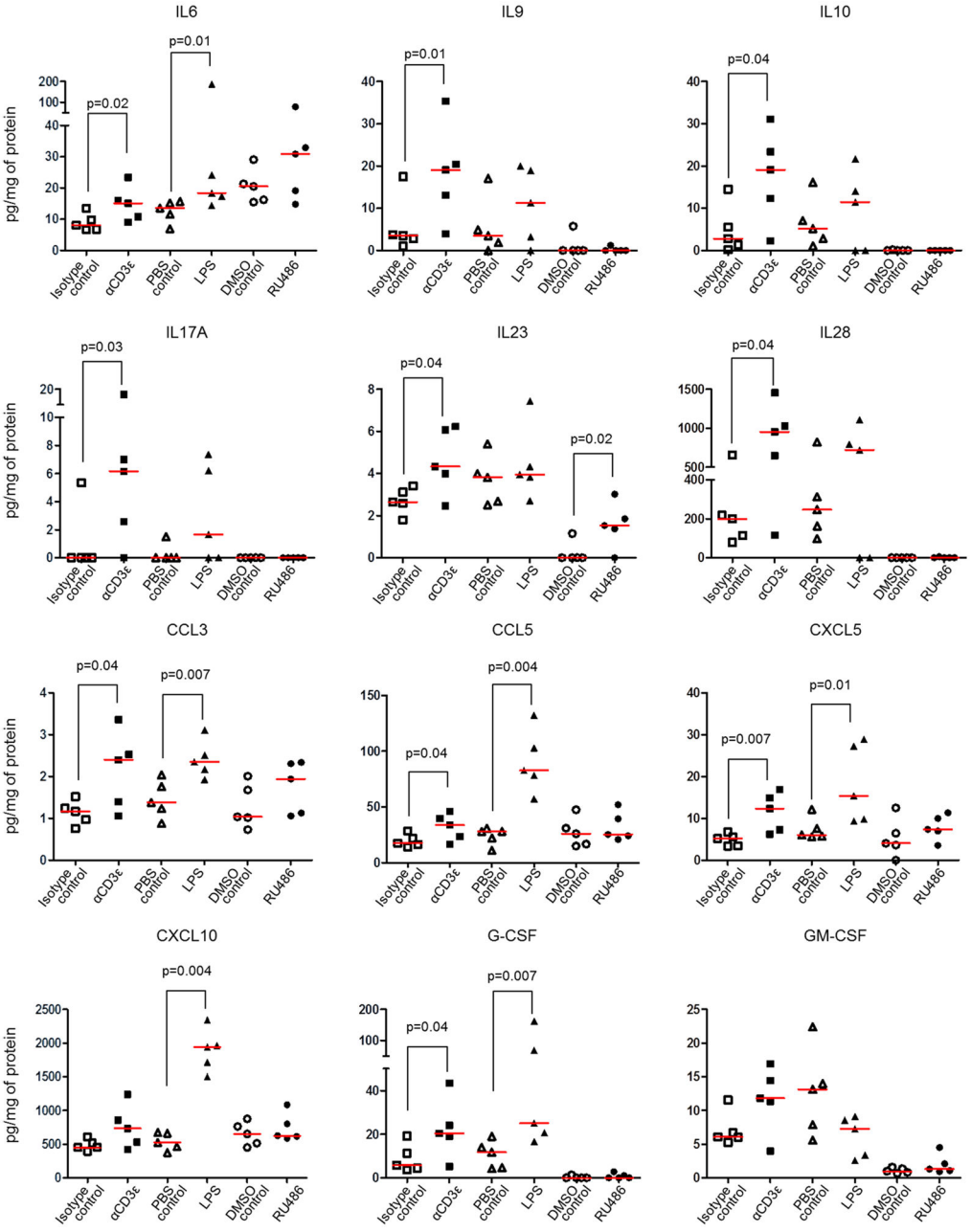

Fig. 7. The fetal inflammatory response prior to preterm birth.

Dams were injected with αCD3ε (or isotype control), LPS (or PBS control), or RU486 (or DMSO control). Concentrations of IL6, IL9, IL10, IL17A, IL23, IL28, CCL3, CCL5, CXCL5, CXCL10, G-CSF, and GM-CSF in amniotic fluid were determined using a cytokine multiplex assay (n=5 each). The p-values were determined by 2-tailed Mann-Whitney U-test. Data are shown as scatter plots (median).

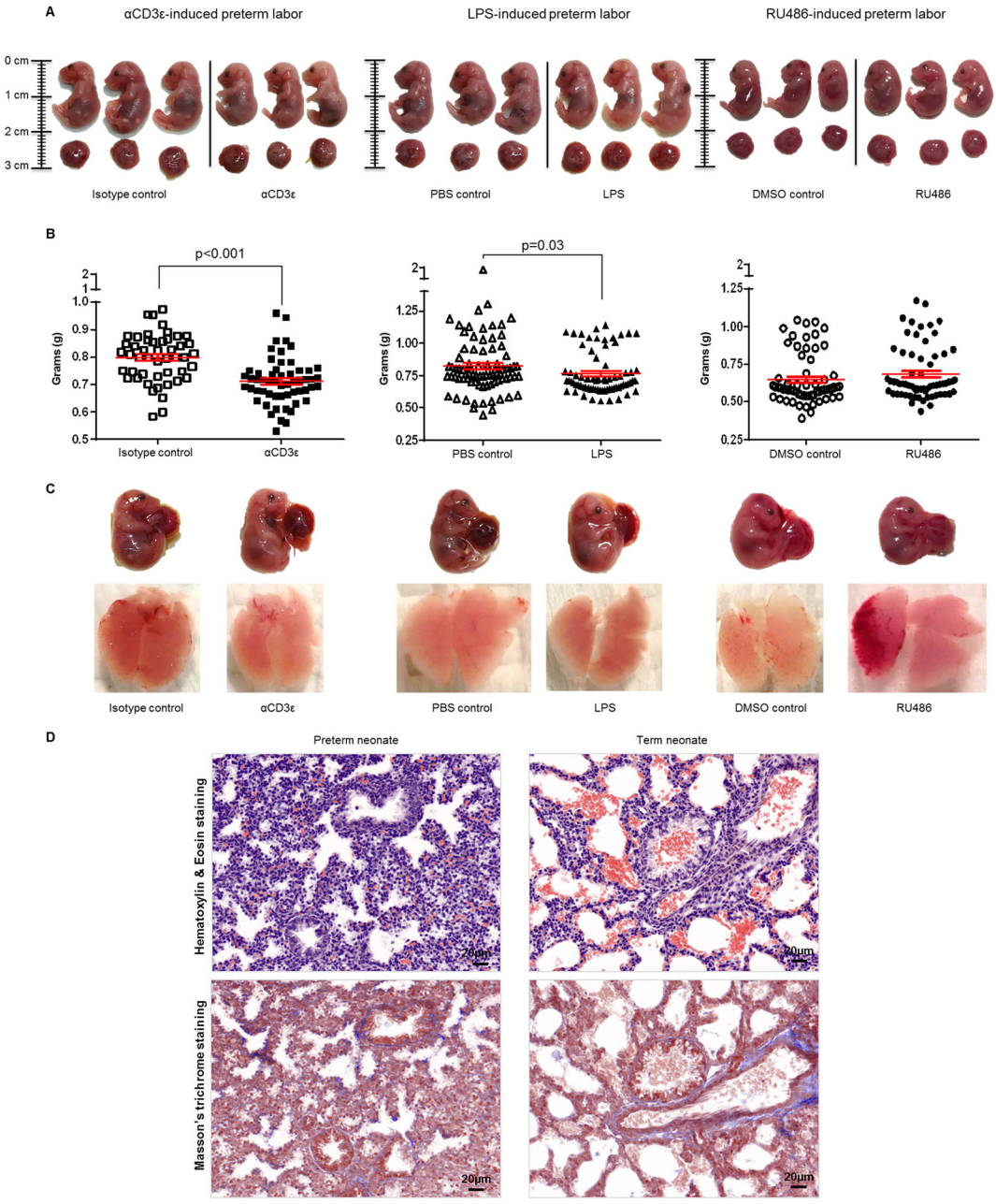

Fig. 8. Fetal growth parameters prior to preterm birth.

(**A**) Fetuses (with their placentas) from dams injected with αCD3ε, LPS, or RU486 or their respective controls prior to preterm birth. Data are representative of individual litters (n=3 each). (**B**) Weights of fetuses from dams injected with αCD3ε, LPS, or RU486 or their respective controls prior to preterm birth (n=7-10 each). The p-values were determined by 2-tailed unpaired *t*-test. Data are shown as scatter plots (mean ± SEM). (**C**) Fetal lungs collected from dams injected with αCD3ε, LPS, or RU486 or their respective controls prior to preterm birth (n=3 each). (**D**) Hematoxylin and eosin (H&E) and Masson's trichrome staining of lungs from preterm and term neonates (n=3 each). Magnification 40x.

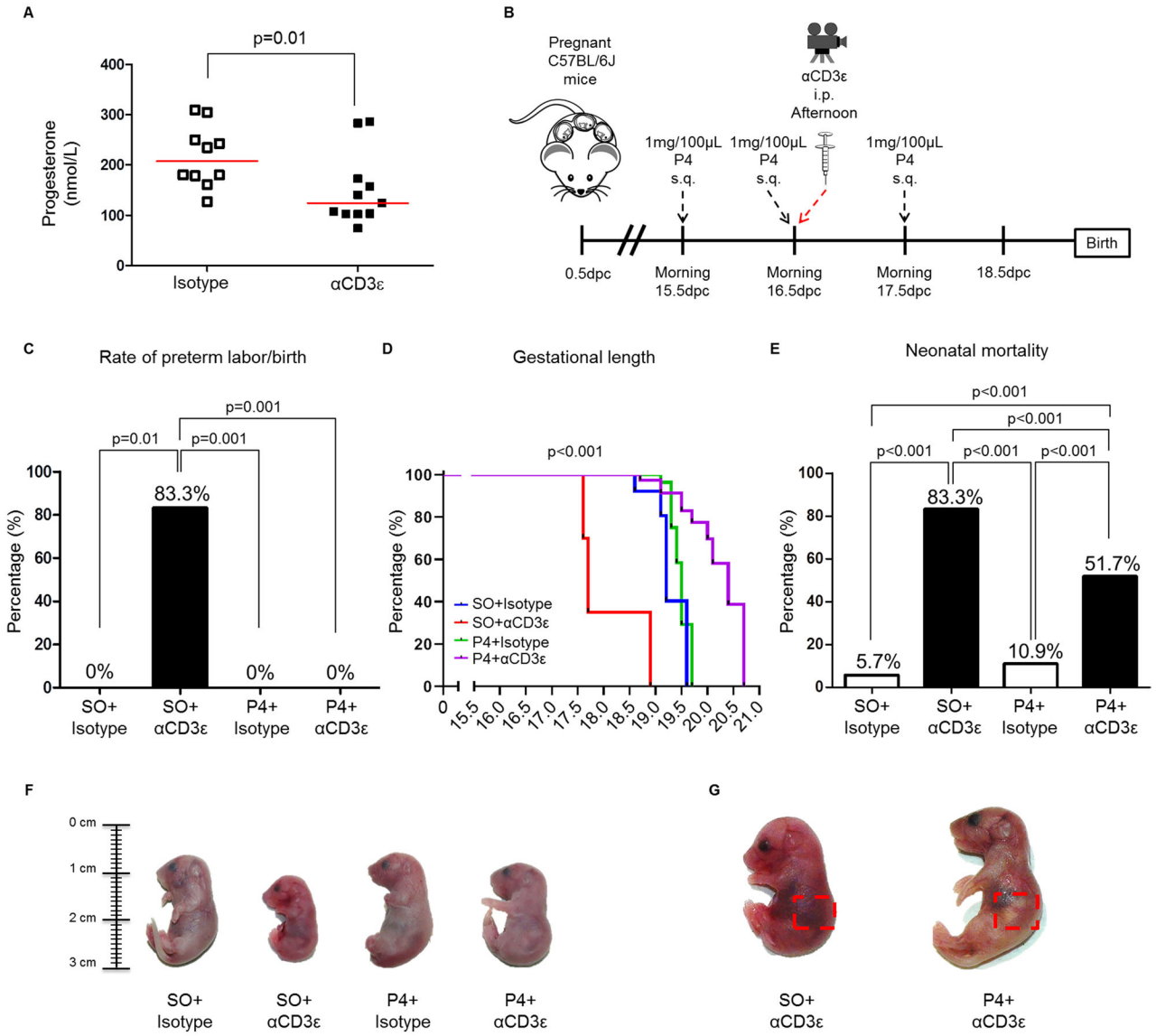

Fig. 9. Progesterone prevents *in vivo* T-cell activation-induced preterm labor/birth and reduces adverse neonatal outcomes.

(**A**) Systemic progesterone (P4) concentration in dams injected with αCD3ε (or isotype control) (n=10-11 each). The p-value was determined by 2-tailed Mann-Whitney *U*-test. (**B**) Scheme of treatment with P4: dams were treated with either P4 or sesame oil (SO), injected with either αCD3ε or isotype control and video monitored until delivery(n= 5-10 each). (**C**) The rate of preterm birth in dams injected with SO+Isotype, SO+αCD3ε, P4+Isotype or P4+αCD3ε (n=5-10 each). The p-values were determined by 2-tailed Fisher's exact test. (**D**) Gestational length and (**E**) the rate of neonatal mortality from pups born to dams injected with SO+Isotype, SO+αCD3ε, P4+Isotype or P4+αCD3ε (n=5-10 each). The p-values were determined by (D) Mantel-Cox test (all comparisons p≤0.001) or (E) 2-tailed Fisher's exact test. (**F**) Representative images of neonates born to dams injected with SO +Isotype, SO+αCD3ε, P4+Isotype or P4+αCD3ε (n=3 each). (**G**) Representative images of

neonates born to dams injected with SO+αCD3ε (left) or P4+αCD3ε (right). Red dashed rectangle indicates the location of the milk band (n=3 each).

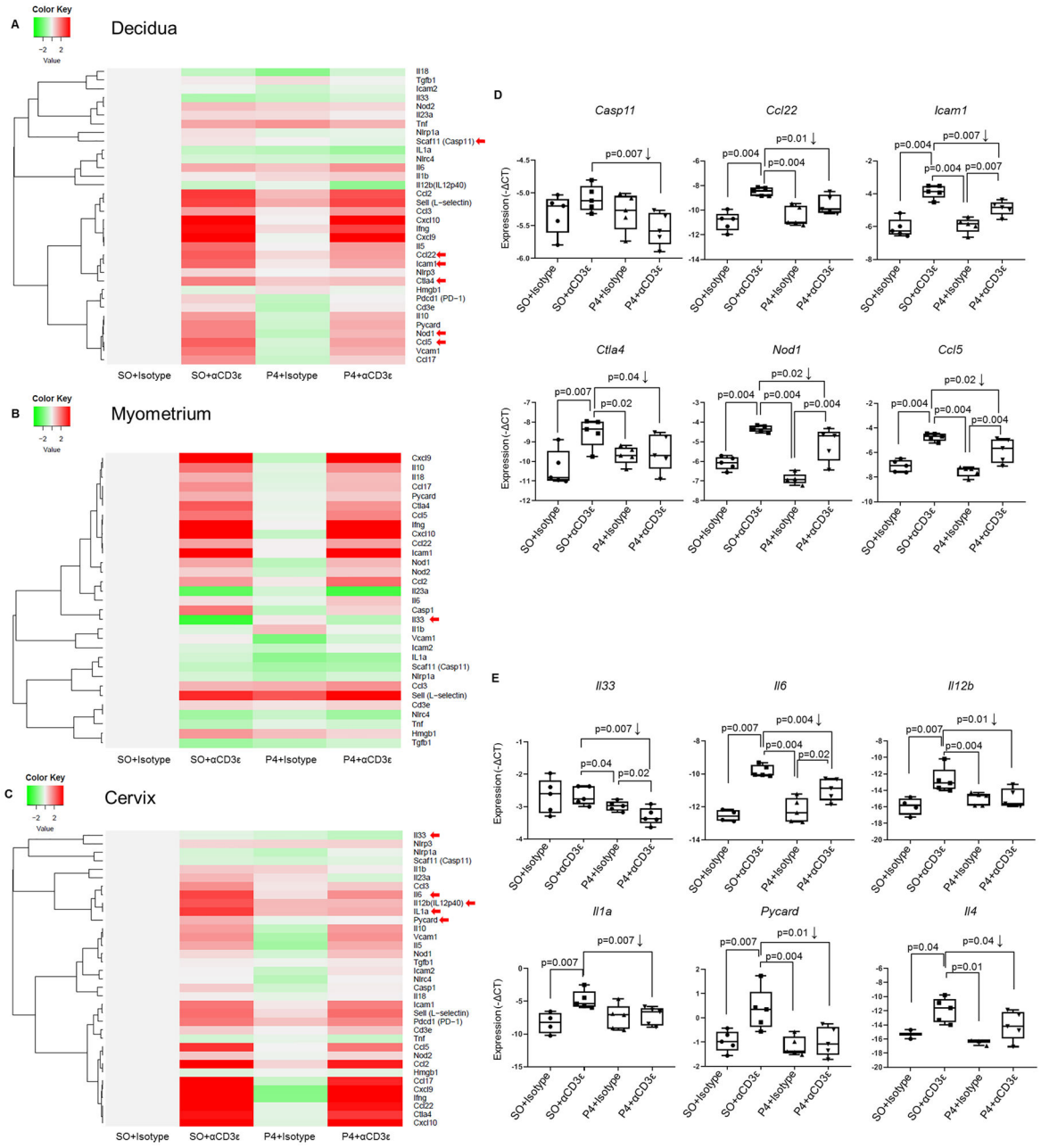

Fig. 10. Progesterone prevents *in vivo* T-cell activation-induced preterm labor/birth by downregulating inflammatory gene expression at the maternal-fetal interface and in the cervix.

Decidual, myometrial and cervical tissues from dams injected with sesame oil (SO)+Isotype, SO+αCD3ε, progesterone (P4)+Isotype or P4+αCD3ε (n=5 each). Heat map visualization of inflammatory gene expression in the (**A**) decidual, (**B**) myometrial, and (**C**) cervical tissues. The–ΔCt values of each group were centered on the −ΔCt value of the control group treated with sesame oil (SO) + Isotype. (**D&E**) Messenger (m)RNA expression of selected genes in decidual and cervical tissues. Negative (−)ΔCt values were calculated using *Actb*, *Gusb*, *Gapdh* and *Hsp90ab1* as reference genes. Red arrows alongside the heat maps indicate

the genes chosen for plotting. Data are from individual dams (n=5 each). The p-values were determined by one-tailed Mann Whitney *U*-test. Data are shown as scatter plots (median).

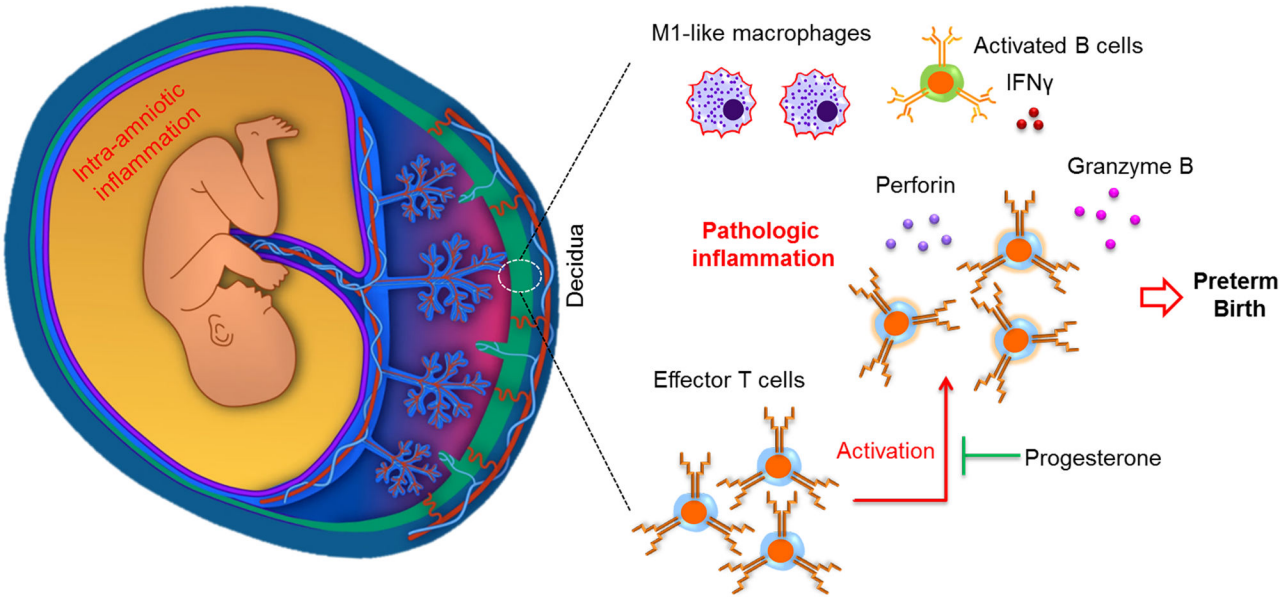

Fig. 11. Conceptual framework.

Maternal effector and activated T cells expressing granzyme B and perforin can induce pathologic inflammation by initiating local immune responses at the maternal-fetal interface (decidua) (i.e. activation of B cells and an M1-like macrophage polarization without an increased influx of neutrophils) which, in turns, leads to preterm labor and birth. Activation of T cells also induces inflammatory responses in the maternal circulation and the amniotic cavity, inducing fetal damage prior to preterm labor and birth. These effects can be abrogated by treatment with the anti-inflammatory and clinically approved strategy, progesterone.

Table I.

Demographic and clinical characteristics of the study population for immunophenotyping of effector memory T cells

	TNL (n=20)	TIL (n=55)	PTNL (n=15)	PTL (n=50)	p value
Age (y; median [IQR])[a]	27 (24-29.3)	25 (22-29)	29 (24.5-35.5)	23 (21.3-26.3)	0.01
Body mass index (kg/m^2; median [IQR])[a]	27.6 (24.5-29.7)	29.3 (24.6-34)	27.5 (24.9-35.8)	24.9 (21.6-29.3)	0.03
Gestational age at delivery (wk; median [IQR])[a]	39.1 (39-39.3)	39.4 (38.6-40.7)	33.9 (28.9-36.3)	34.2 (31.2-35.9)	<0.001
Birth weight (g; median [IQR])[a]	3232.5 (2911.3-3658.8)	3205 (3007.5-3506.3)	1930 (1082.5-2385)	1977.5 (1466.3-2343.8)	<0.001
Race (n[%])[b]					0.004
African-American	13 (65%)	51 (92.7%)	11 (73.3%)	44 (88%)	
Caucasian	3 (15%)	3 (5.5%)	3 (20%)	1 (2%)	
Hispanic	2 (10%)	0 (0%)	0 (0%)	0 (0%)	
Asian	2 (10%)	0 (0%)	0 (0%)	2 (4%)	
Other	0 (0%)	1 (1.8%)	1 (6.7%)	3 (6%)	
Primiparity (n[%])[b]	2 (10%)	7 (12.7%)	3 (20%)	11 (22%)	NS
Cesarean section (n[%])[b]	20 (100%)	6 (10.9%)	15 (100%)	9 (18%)	<0.001

[a] Kruskal-Wallis test;

[b] Fisher's exact test;

IQR = interquartile range, TNL = term no labor, TIL = term in labor, PTNL = preterm no labor, PTL = preterm in labor

Table II.

Demographic and clinical characteristics of the study population for immunophenotyping of activated T cells

	TNL (n=20)	TIL (n=37)	PTNL (n=18)	PTL (n=53)	p value
Age (y; median [IQR])[a]	24 (22-30.3)	26 (22-31)	30 (26-33)	24 (20-29)	0.02
Body mass index (kg/m^2; median [IQR])[a]	33.7 (27.2-37.1)	28.5 (24.2-35.6)	27.8 (24-35.4)	26.4 (21.5-31.3)	NS
Gestational age at delivery (wk; median [IQR])[a]	39 (38.8-39.3)	38.9 (38.3-39.4)	33.4 (30.5-34.4)	34.9 (33.9-35.7)	<0.001
Birth weight (g; median [IQR])[a]	3355 (2872.5-3511.3)	3185 (2735-3495)	1420 (1205.3-2095)	2255 (1830-2540)	<0.001
Race (n[%])[b]					NS
African-American	15 (75%)	35 (94.6%)	12 (66.6%)	46 (86.8%)	
Caucasian	3 (15%)	1 (2.7%)	4 (22.2%)	5 (9.4%)	
Hispanic	0 (0%)	0 (0%)	0 (0%)	0 (%)	
Asian	1 (5%)	0 (0%)	1 (5.6%)	0 (%)	
Other	1 (5%)	1 (2.7%)	1 (5.6%)	2 (3.8%)	
Primiparity (n[%])[b]	0 (0%)	10 (27%)	3 (16.7%)	14 (26.4%)	0.03
Cesarean section (n[%])[b]	20 (100%)	4 (10.8%)	18 (100%)	12 (22.6%)	<0.001

[a]Kruskal-Wallis test;

[b]Fisher's exact test;

IQR = interquartile range, TNL = term no labor, TIL = term in labor, PTNL = preterm no labor, PTL = preterm in labor